Electronic Supplementary Material (ESI) for Physical Chemistry Chemical Physics.

Supporting Information

The Windmill, the Dragon, and the Frog: geometry control over the spectral, magnetic, and electrochemical properties of cobalt phthalocyanine regioisomers

Nikolai Tkachenko, Viacheslav Golovanov, Aleksandr Penni, Sami Vesamäki, M. R. Ajayakumar, Atsuya Muranaka, Nagao Kobayashi, and Alexander Efimov

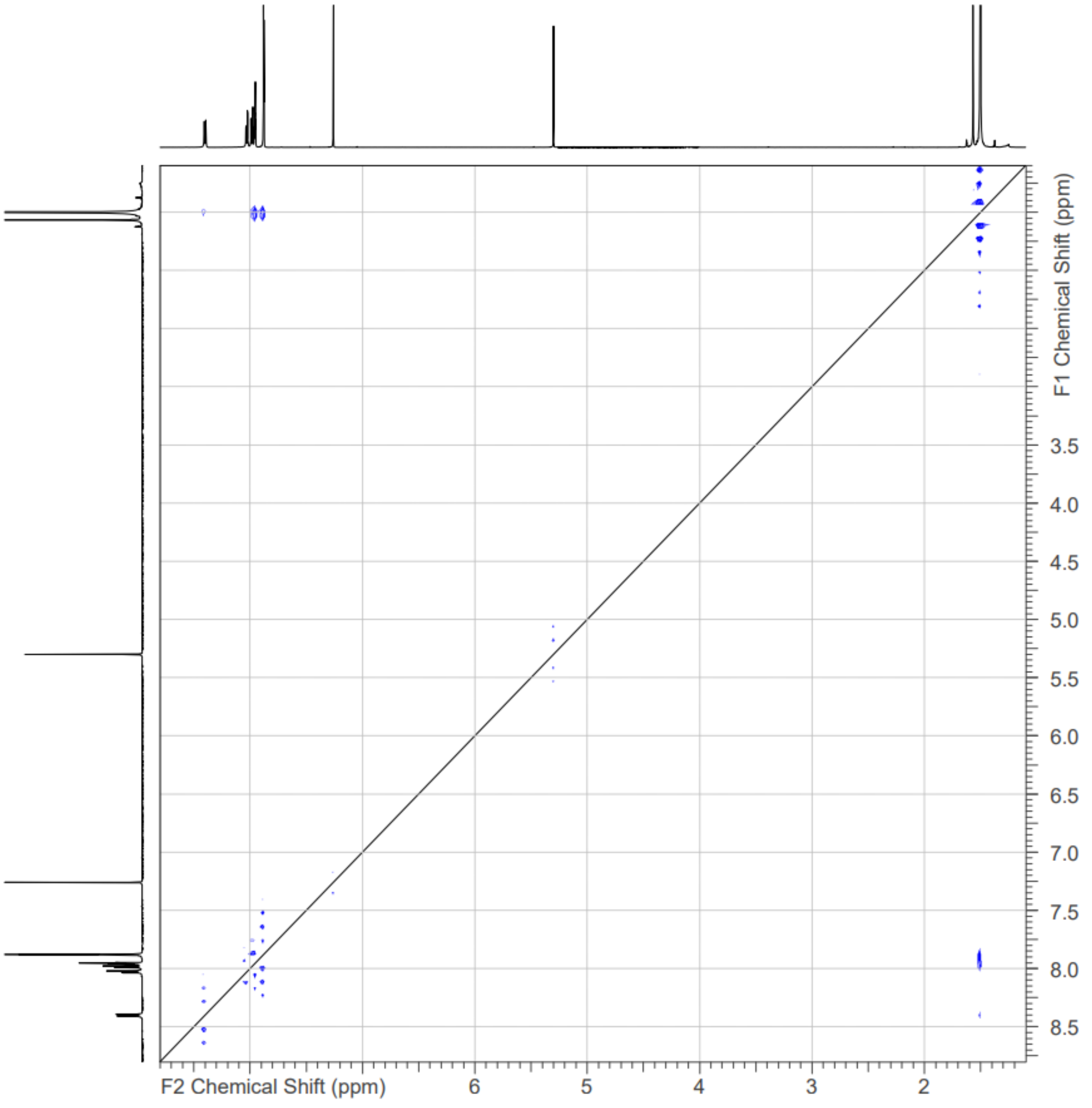

Fig. S1. ^1H–^1H NOESY NMR spectrum (500 MHz, $CDCl_3$) of **H_2Pc-Windmill**.

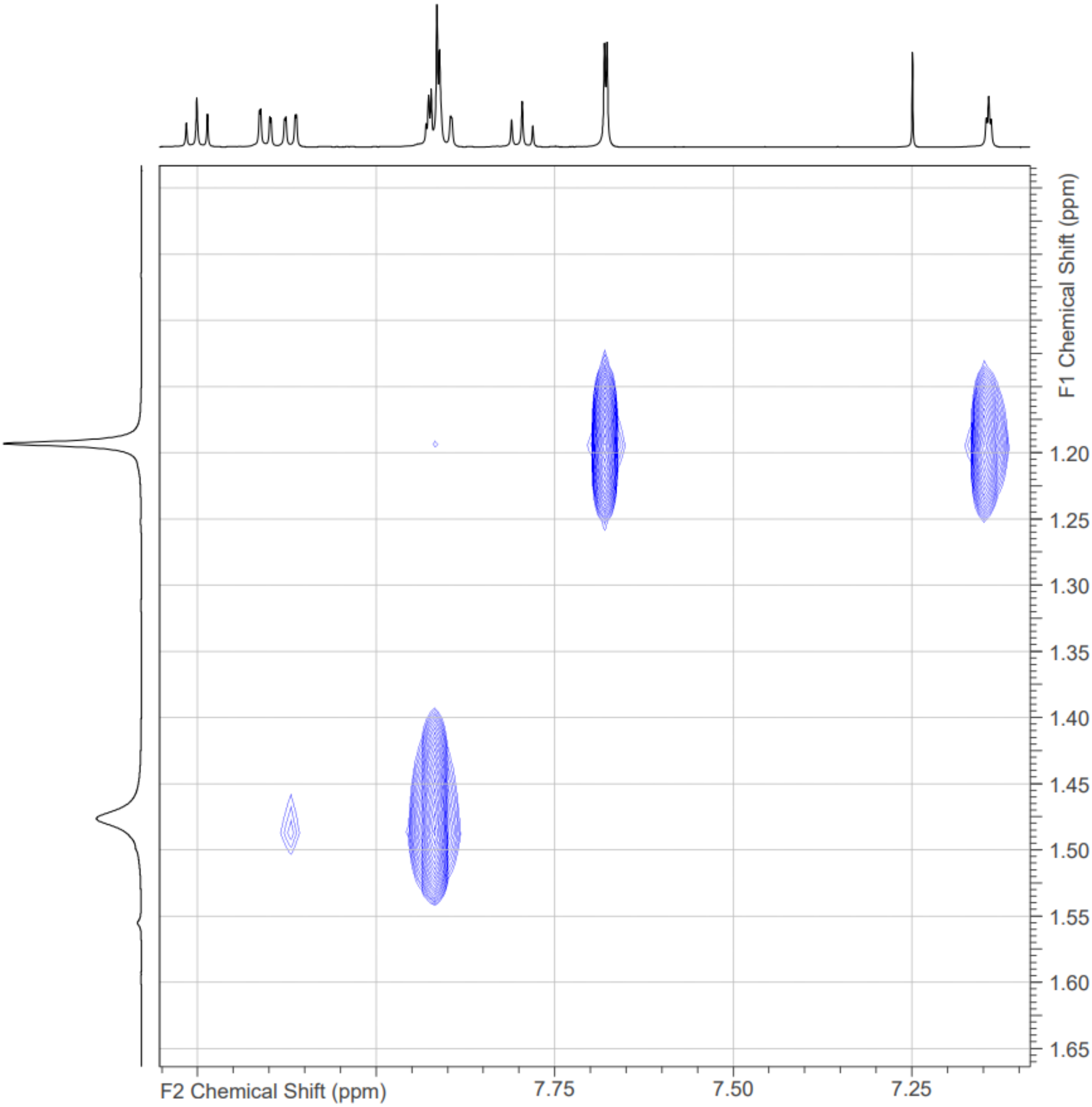

Fig. S2. ^1H–^1H NOESY NMR spectrum (500 MHz, $CDCl_3$) of **H_2Pc-Frog**.

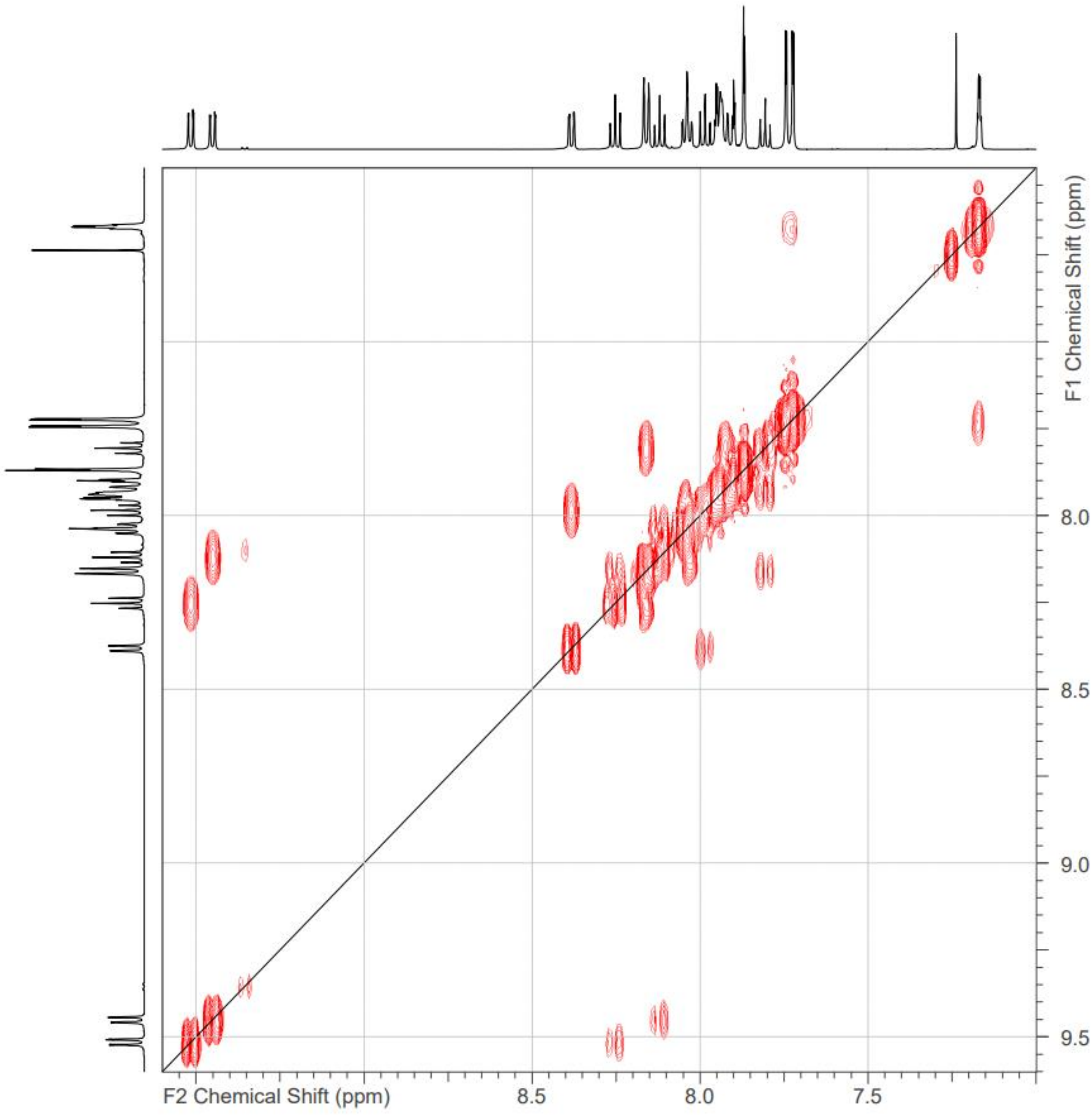

Fig. S3. ^{1}H–^{1}H COSY NMR spectrum (500 MHz, $CDCl_3$) of **H_2Pc-Dragon**.

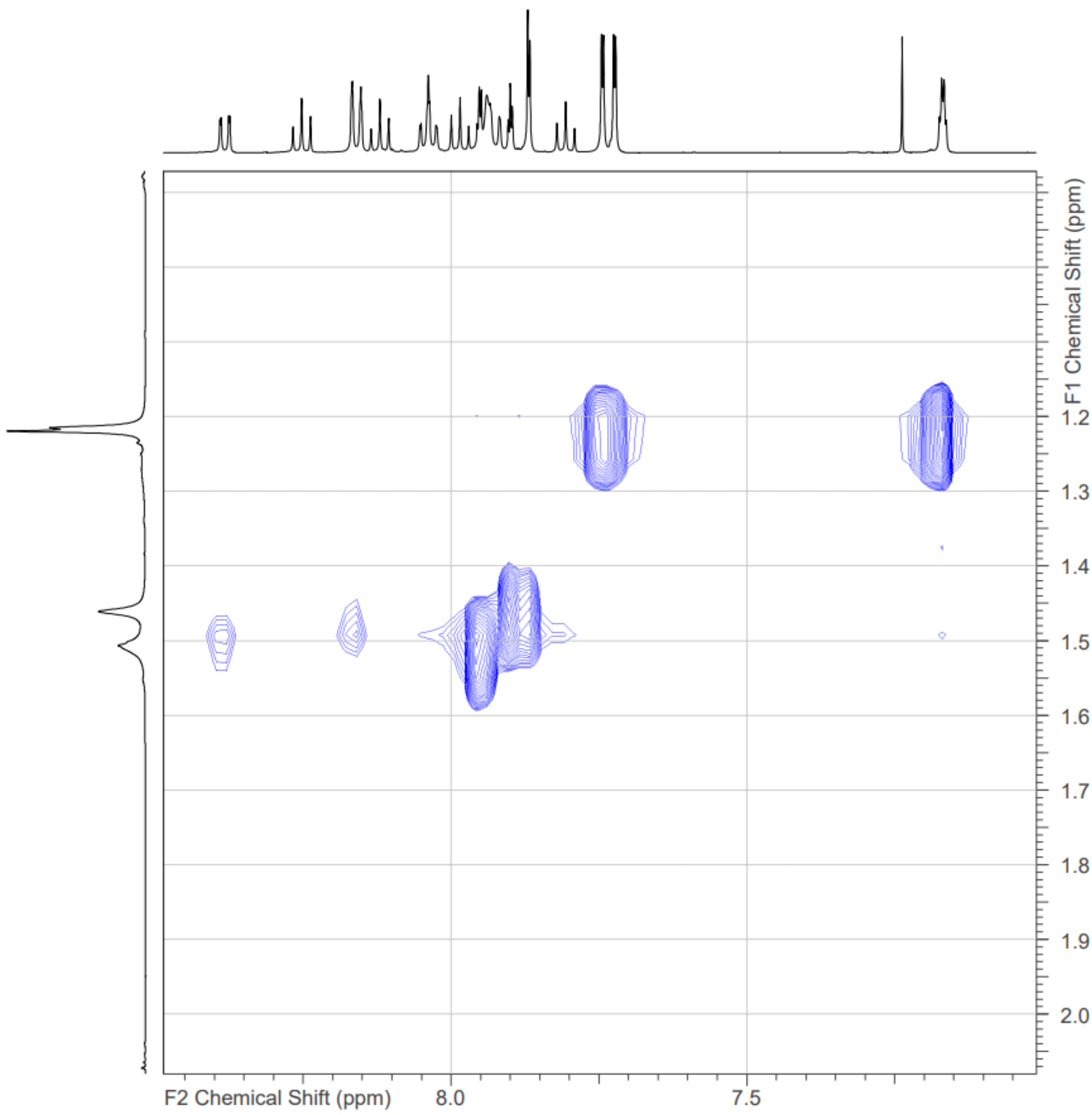

Fig. S4. [1]H–[1]H NOESY NMR spectrum (500 MHz, $CDCl_3$) of **H_2Pc-Dragon**.

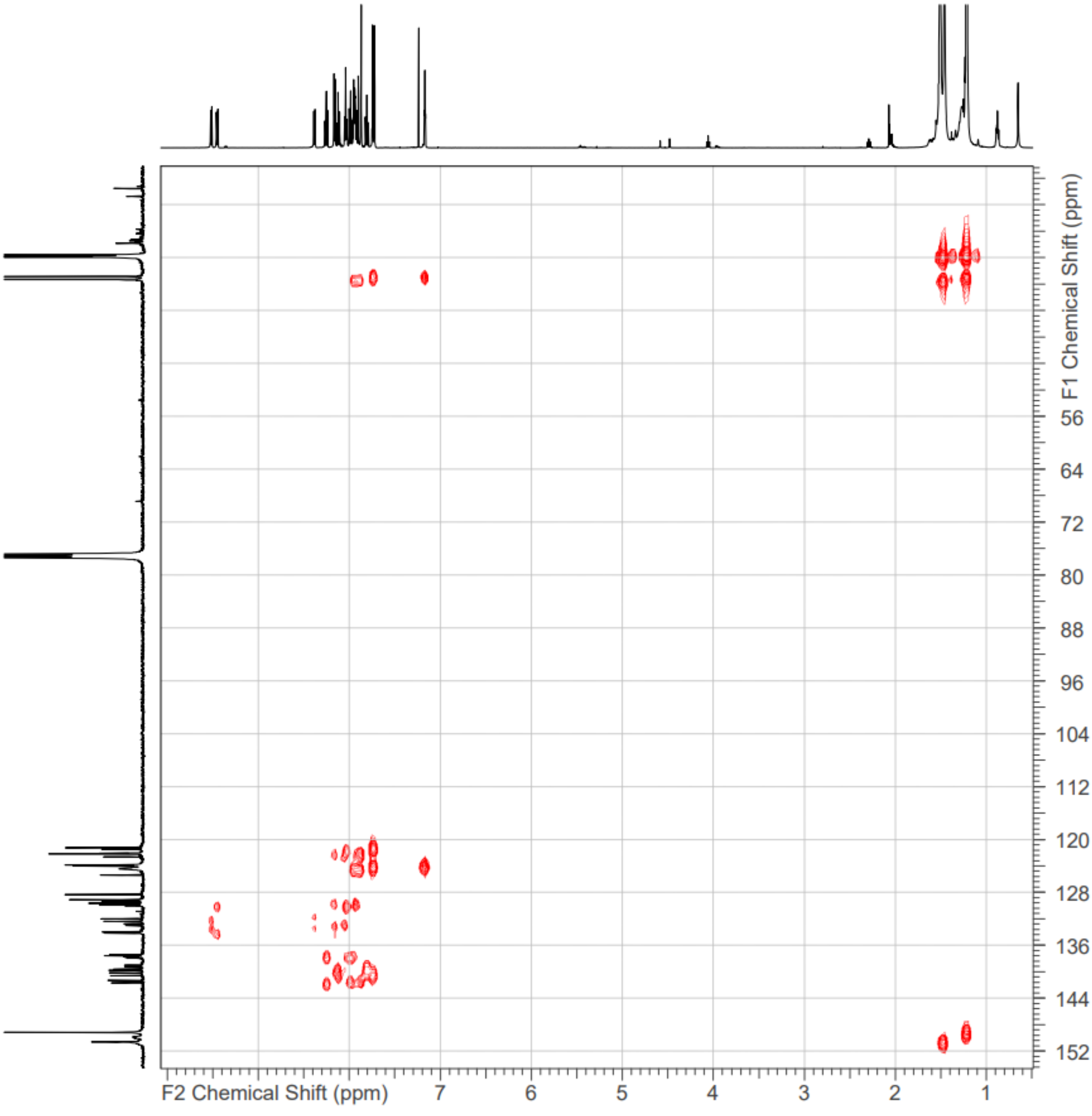

Fig. S5. ^{1}H–^{13}C HMBC NMR spectrum (500 MHz, $CDCl_3$) of **H_2Pc-Dragon**.

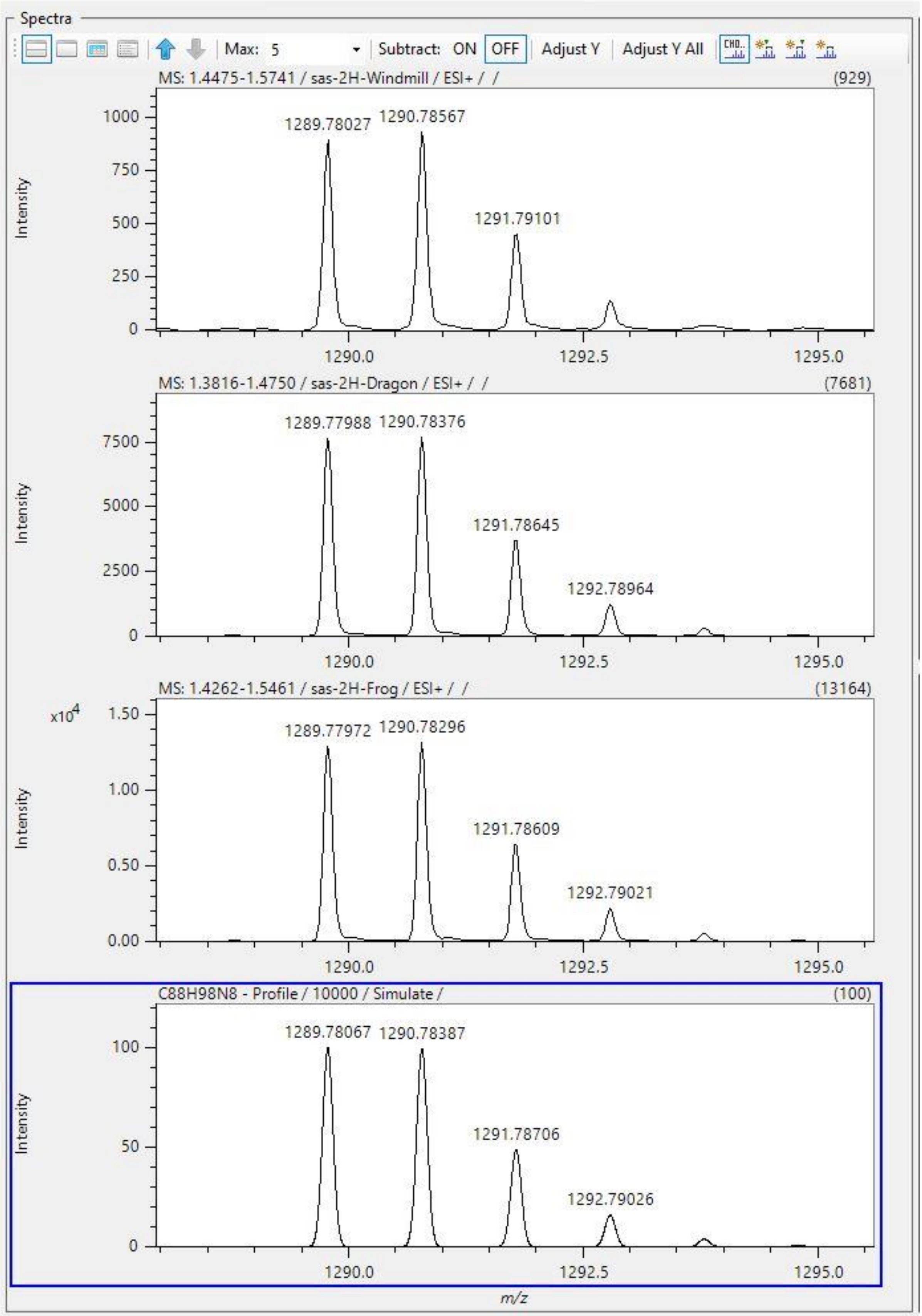

Fig. S6a. High-resolution ESI-TOF mass spectra of **H_2Pc-Windmill**, **H_2Pc-Dragon**, and **H_2Pc-Frog** vs. the $[M+Na]^+$ ($C_{88}H_{98}N_8Na^+$) isotope model (bottom).

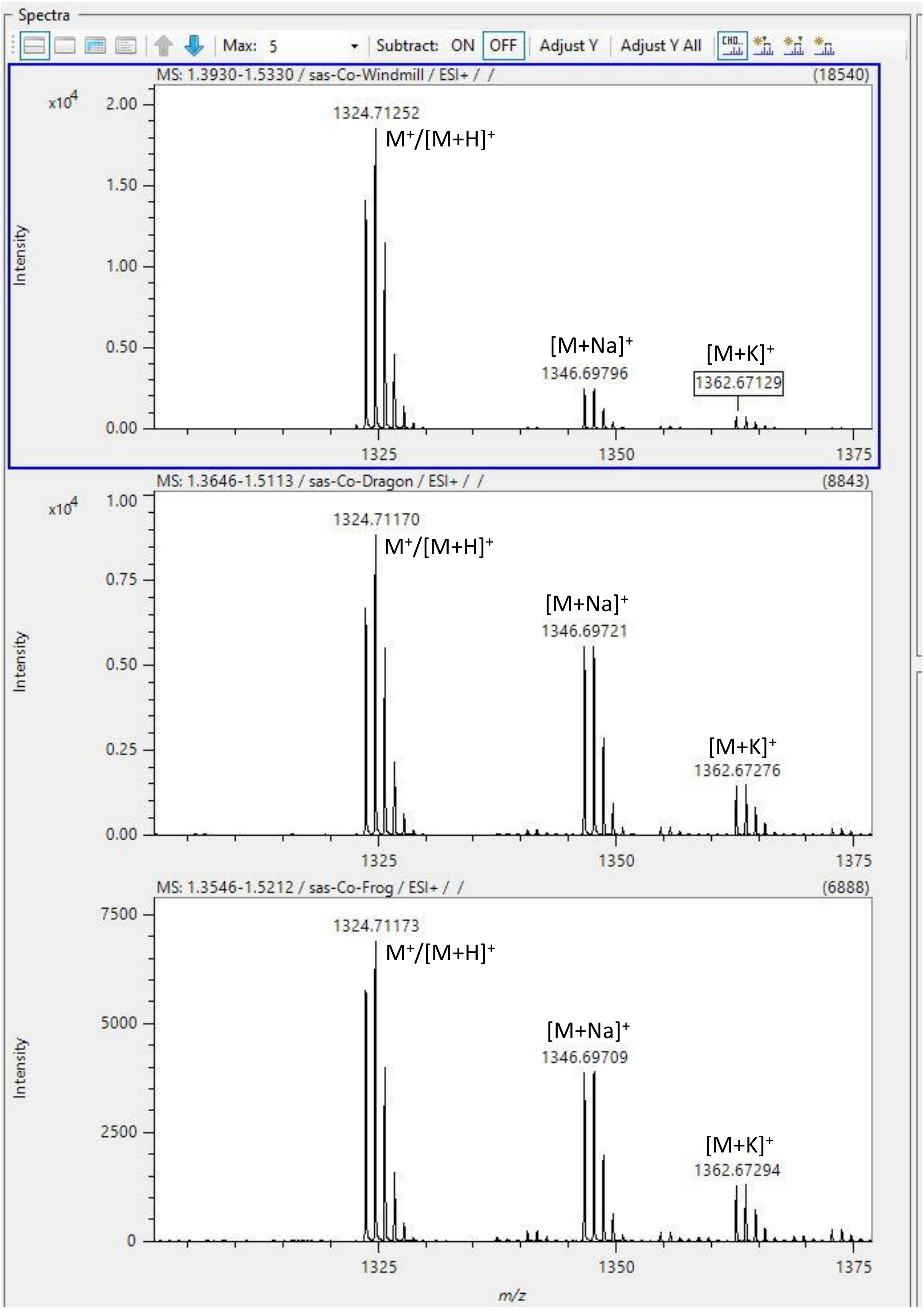

Fig. S6b. High-resolution ESI-TOF mass spectra of **CoPc-Windmill**, **CoPc-Dragon**, and **CoPc-Frog** showing the M^+/$[M+H]^+$, $[M+Na]^+$ and $[M+K]^+$ signals.

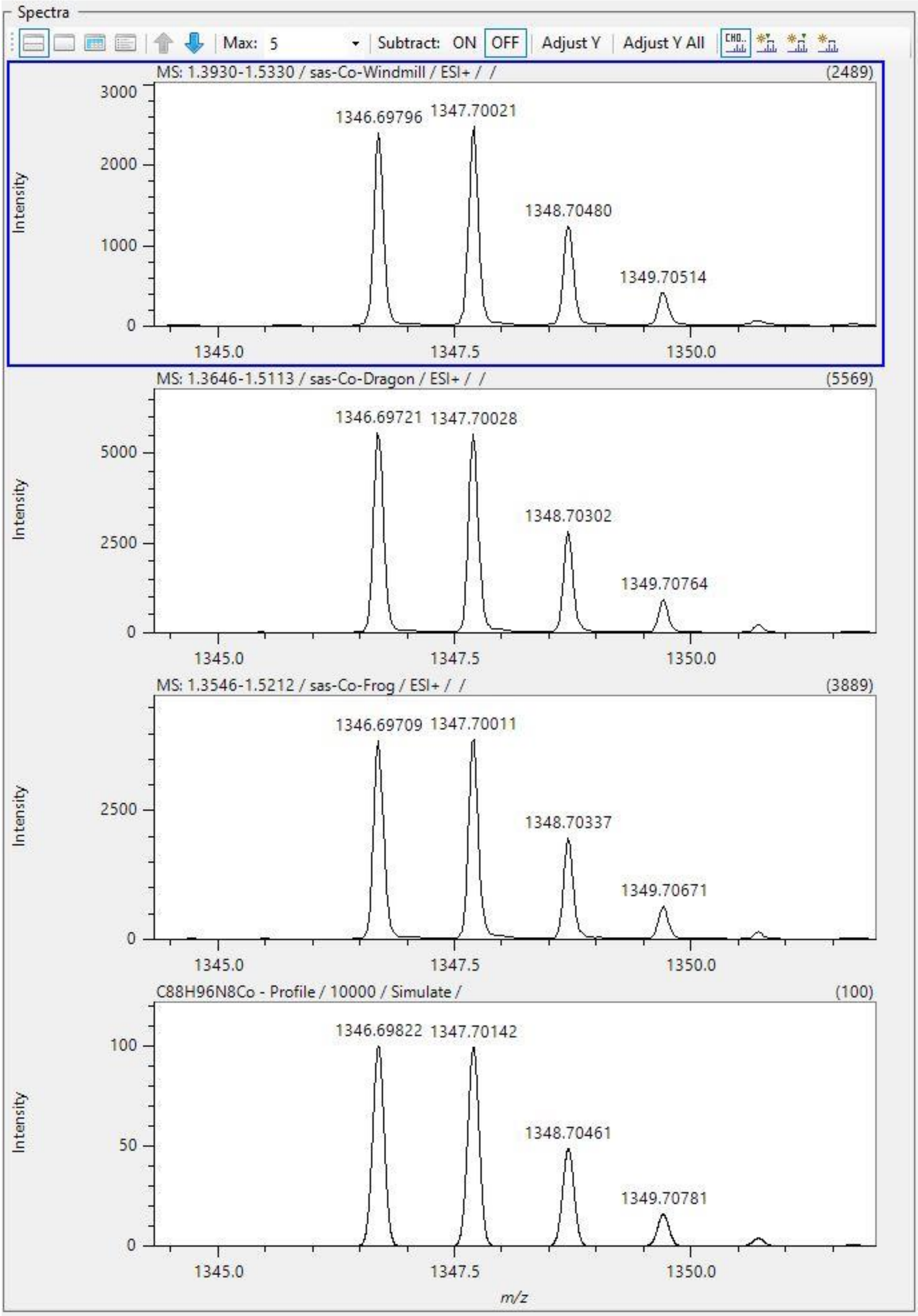

Fig. S6c. High-resolution ESI-TOF mass spectra of **CoPc-Windmill**, **CoPc-Dragon**, and **CoPc-Frog** vs. the $[M+Na]^+$ ($C_{88}H_{96}N_8CoNa^+$) isotope model (bottom).

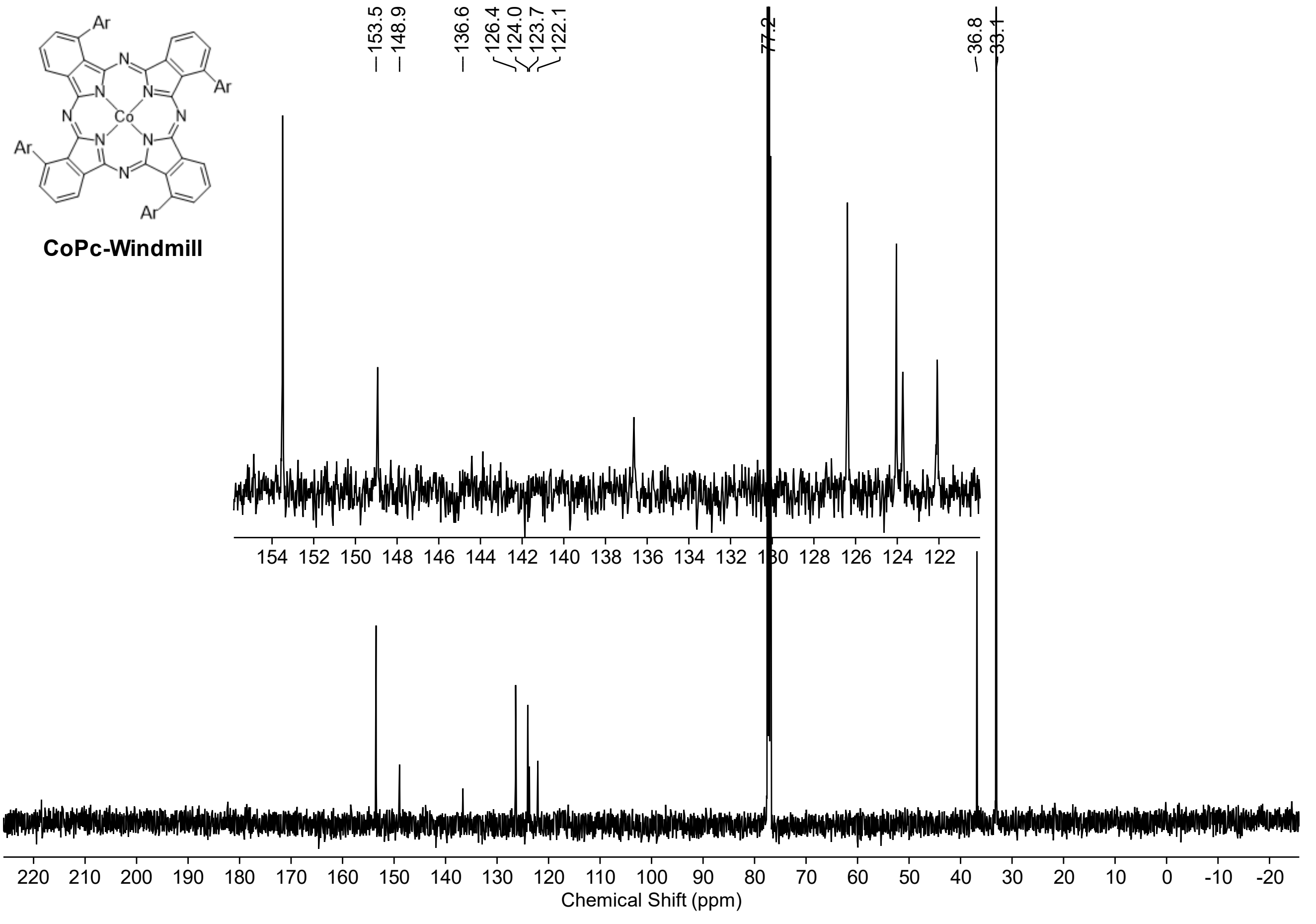

Fig. S7. $^{13}C\{^{1}H\}$ NMR spectrum (126 MHz, $CDCl_3$) of **CoPc-Windmill**.

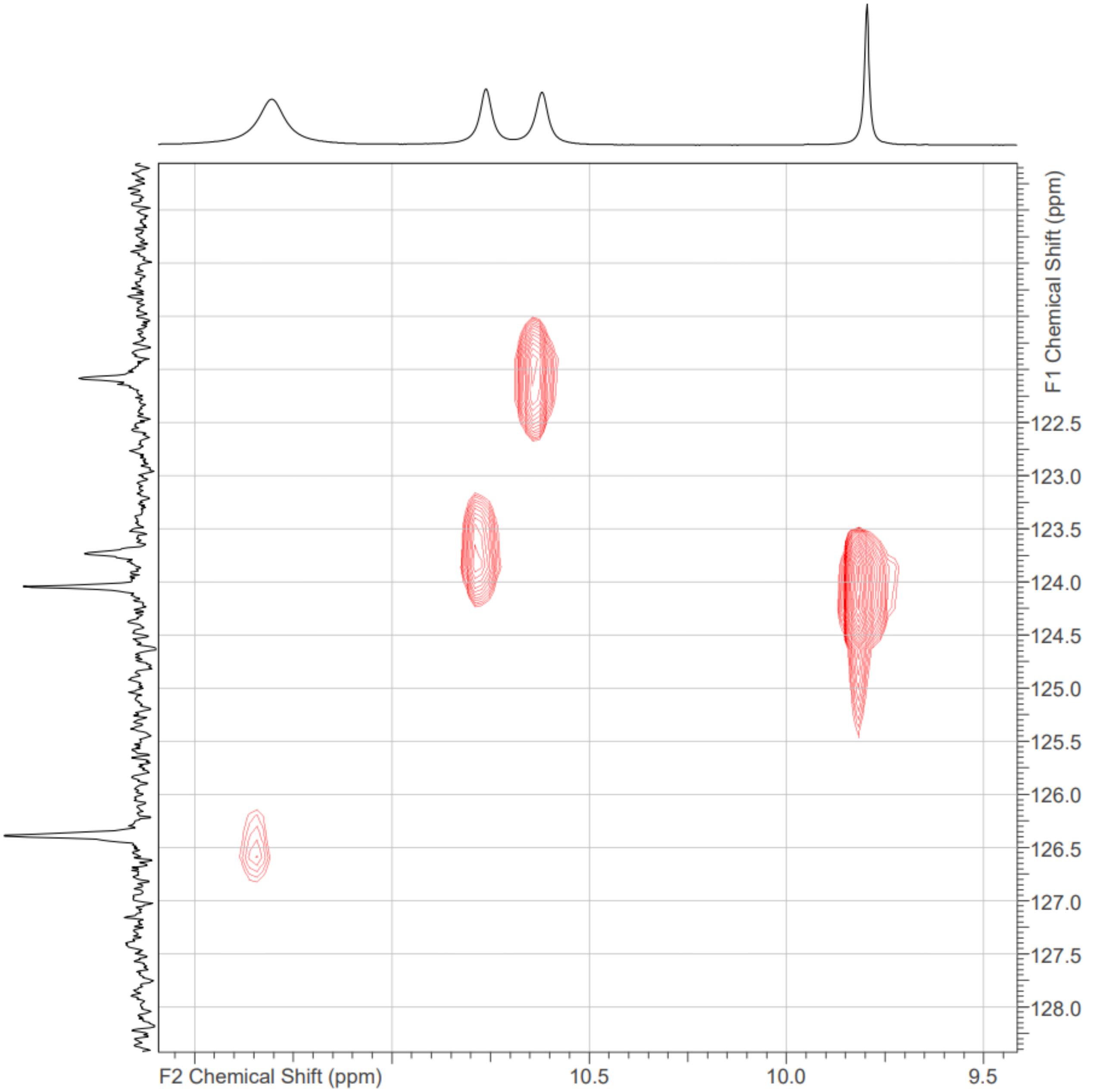

Fig. S8. ^1H–^{13}C HSQC NMR spectrum (500 MHz, $CDCl_3$) of **CoPc-Windmill**.

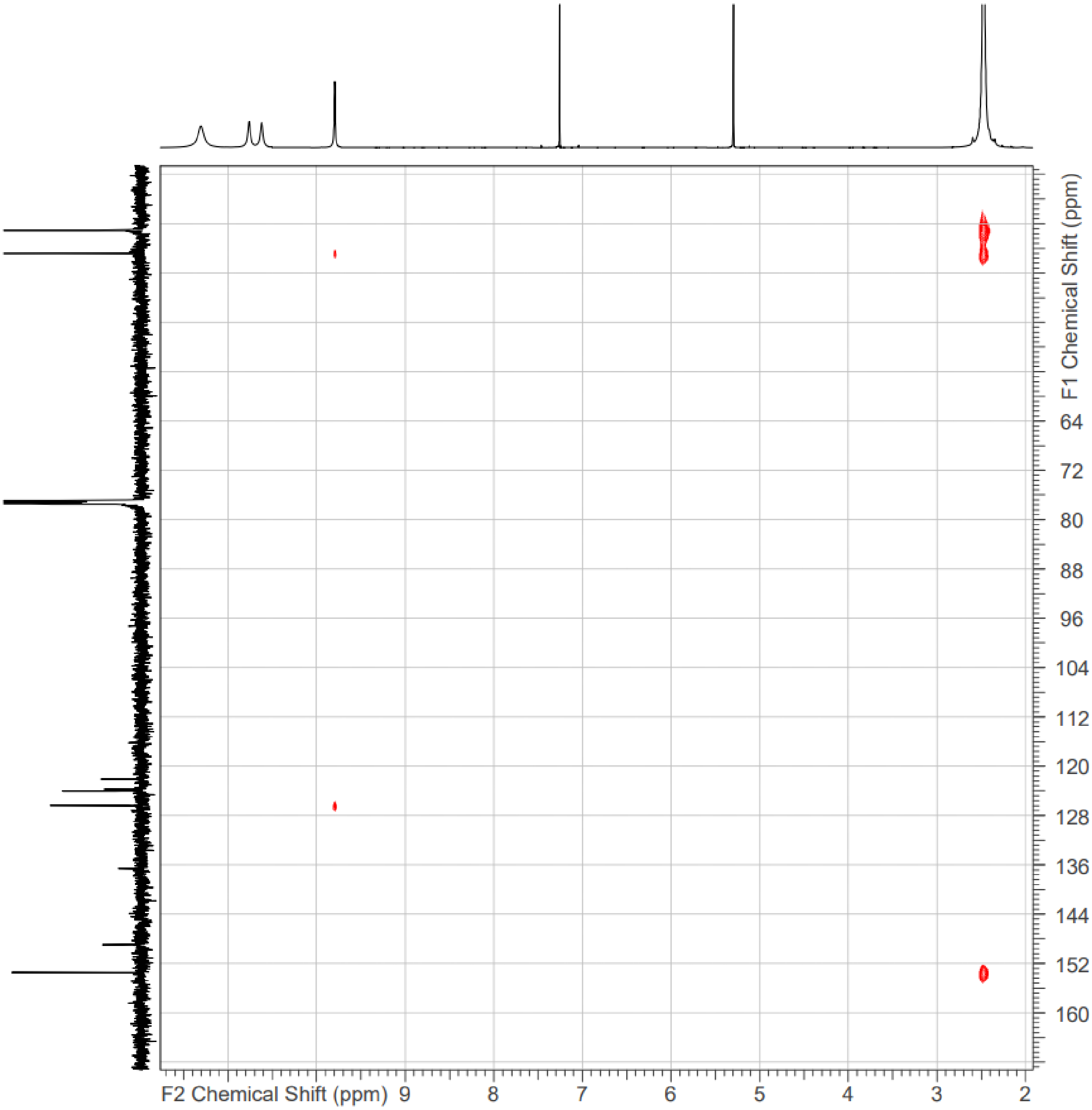

Fig. S9. $^{1}H–^{13}C$ HMBC NMR spectrum (500 MHz, $CDCl_3$) of **CoPc-Windmill**.

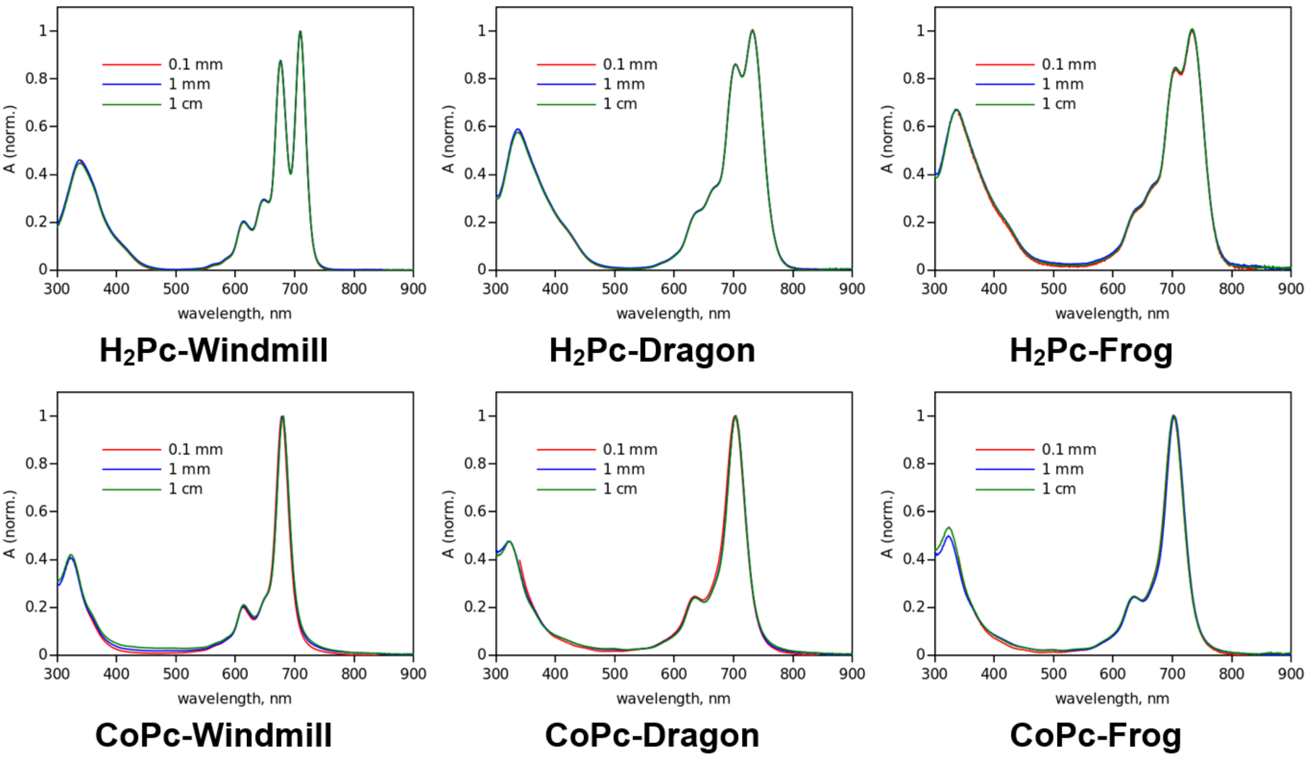

Fig. S10. Normalized absorption spectra of the compounds in chloroform measured at concentrations of approx. 0.01 mM (1 cm cuvette), 0.1 mM (1 mm cuvette) and 1 mM (0.1 mm cuvette).

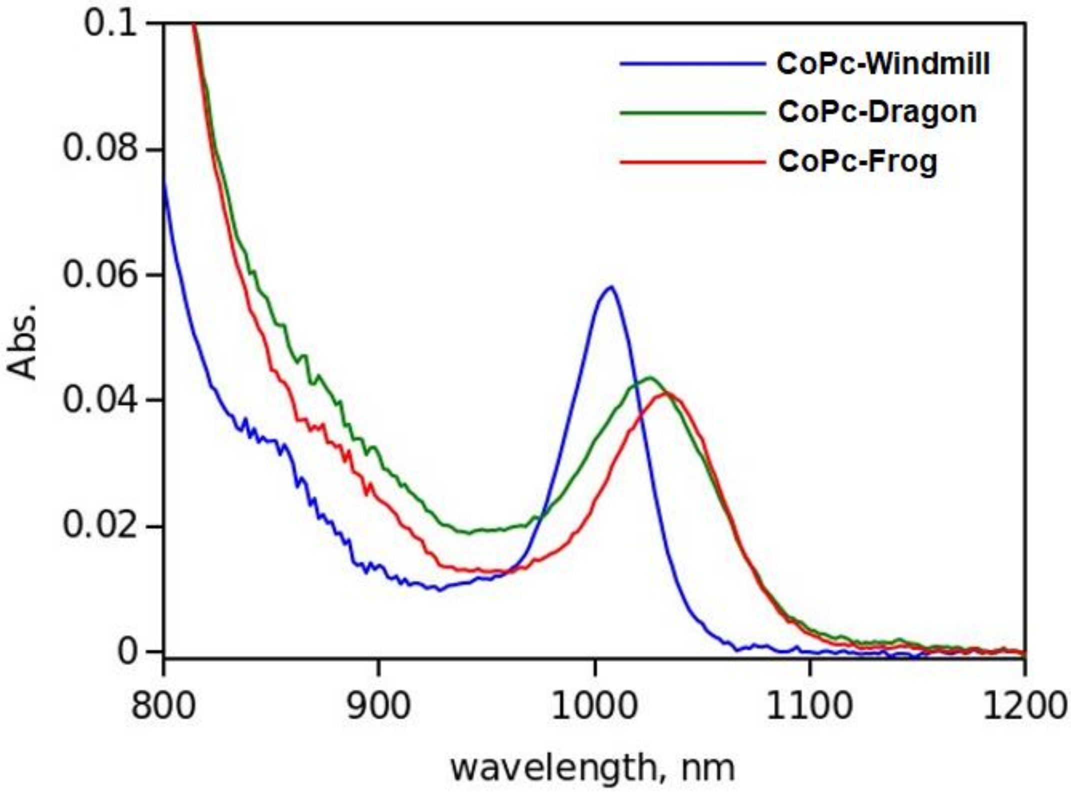

Fig. S11. NIR absorption spectra of **CoPc-Windmill**, **CoPc-Dragon**, and **CoPc-Frog** in toluene.

	H_2Pc-Windmill solution	**H_2Pc-Windmill** film	**H_2Pc-Dragon** solution	**H_2Pc-Dragon** film	**H_2Pc-Frog** solution	**H_2Pc-Frog** film
λ_{max}, nm	708.0	717.1	729.5	740.2	730.1	740.6
$\Delta\lambda_G$, nm	8.1	14.8	14.9	23.8	16.1	24.8
rel. ampl.	2.51	1.29	2.00	1.04	1.90	1.08
λ_{max}, nm	674.8	679.5	696.2	699.4	695.9	699.6
$\Delta\lambda_G$, nm	8.6	11.5	9.6	11.8	9.7	11.9
rel. ampl.	2.14	0.88	1.54	0.46	1.36	0.39
λ_{max}, nm	645.3	649.9	665.9	669.0	665.8	670.1
$\Delta\lambda_G$, nm	12.1	15.9	16.4	17.7	16.8	19.7
rel. ampl.	0.68	0.55	0.67	0.39	0.64	0.39
λ_{max}, nm	612.3	612.6	628.7	633.1	628.6	633.0
$\Delta\lambda_G$, nm	12.3	12.2	12.9	11.7	13.1	11.9
rel. ampl.	0.47	0.35	0.41	0.17	0.38	0.15
λ_{max}, nm		718.8		730.5		736.9
$\Delta\lambda_G$, nm		67.1		125.5		124.8
rel. ampl.		0.28		0.32		0.31

Table S1. Results of the Gaussian fits for the Q band regions of **H_2Pc-Windmill**, **H_2Pc-Dragon**, and **H_2Pc-Frog** as solutions in toluene and films on glass substrates.

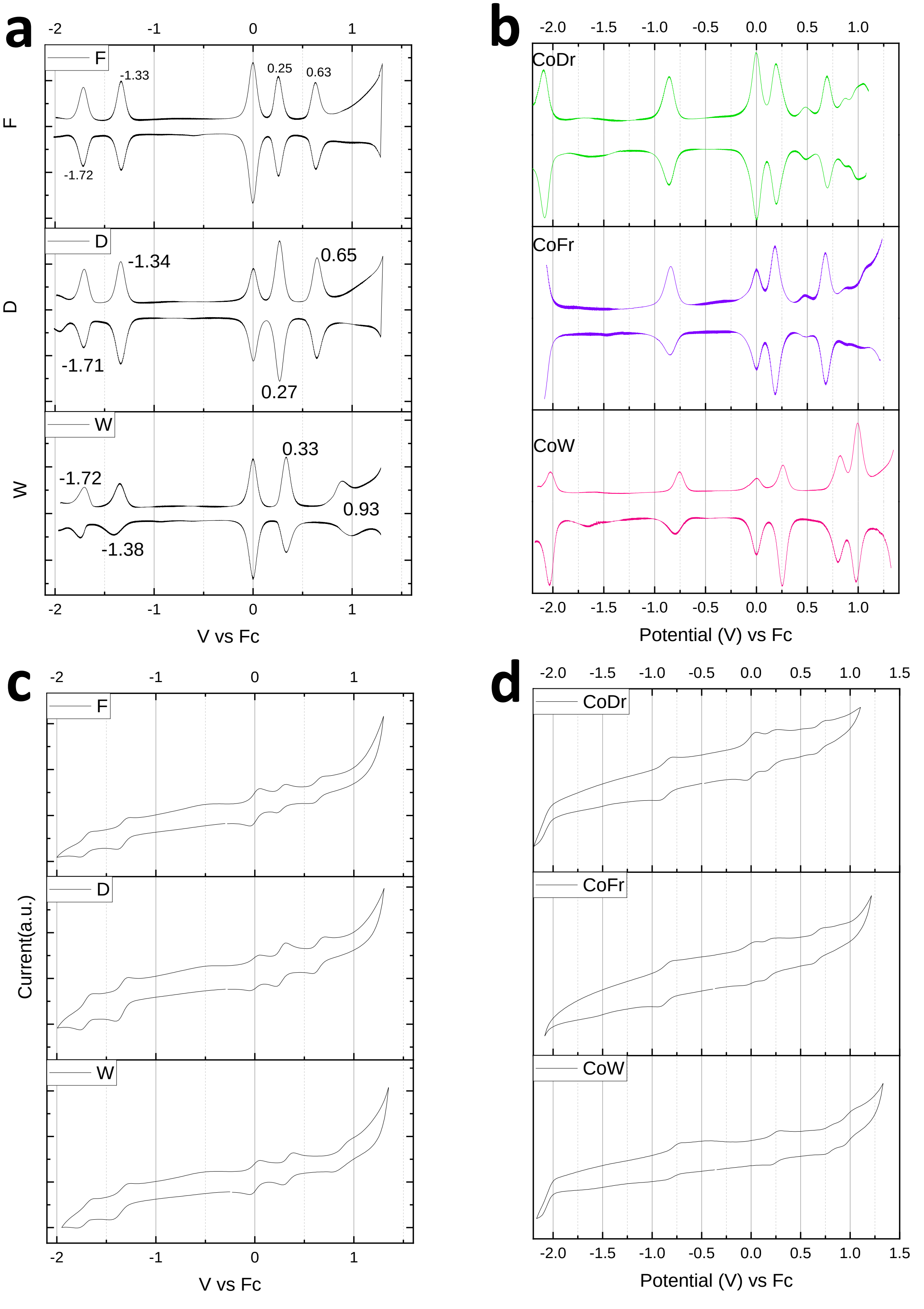

Fig. S12. DPV curves (**a**, **b**) and CV curves (**c**, **d**) for the free base phthalocyanines and Co complexes. Solutions in DCM with Bu_4NPF_6, 200 mV scan rate.

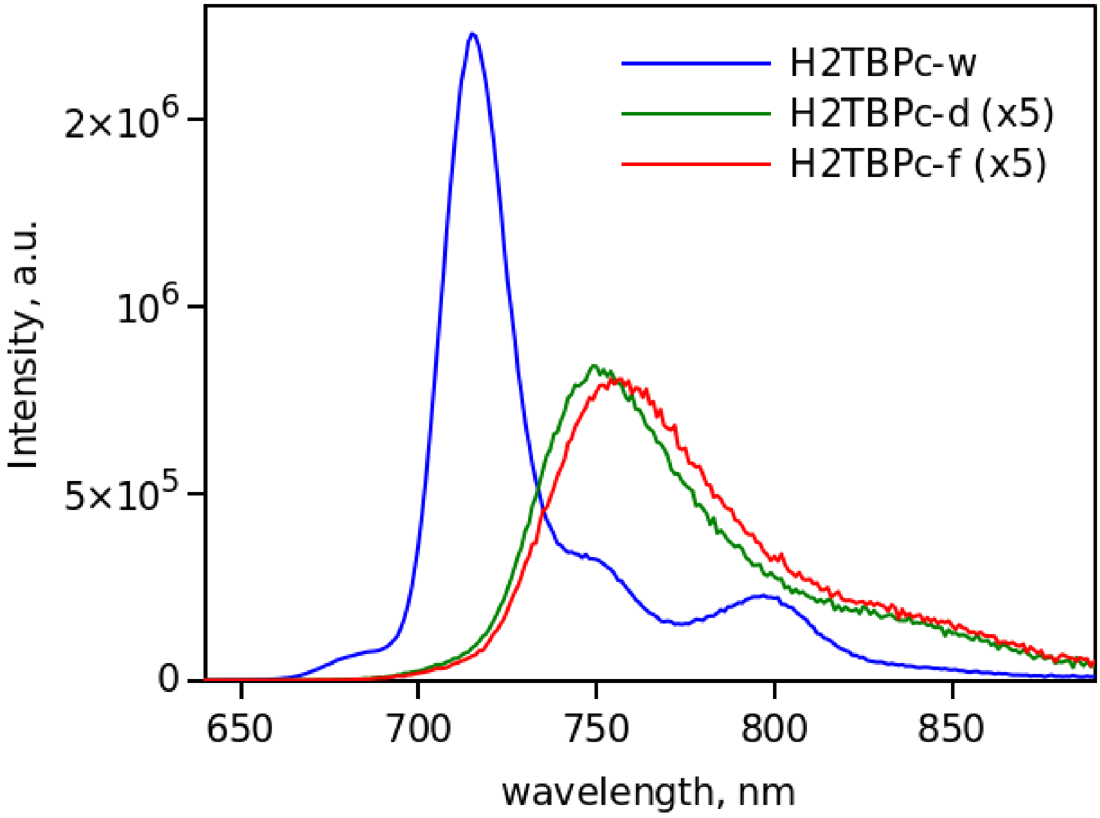

Fig. S13. Emission spectra of **H_2Pc-Windmill**, **H_2Pc-Dragon**, and **H_2Pc-Frog**. Excitation wavelength is 340 nm.

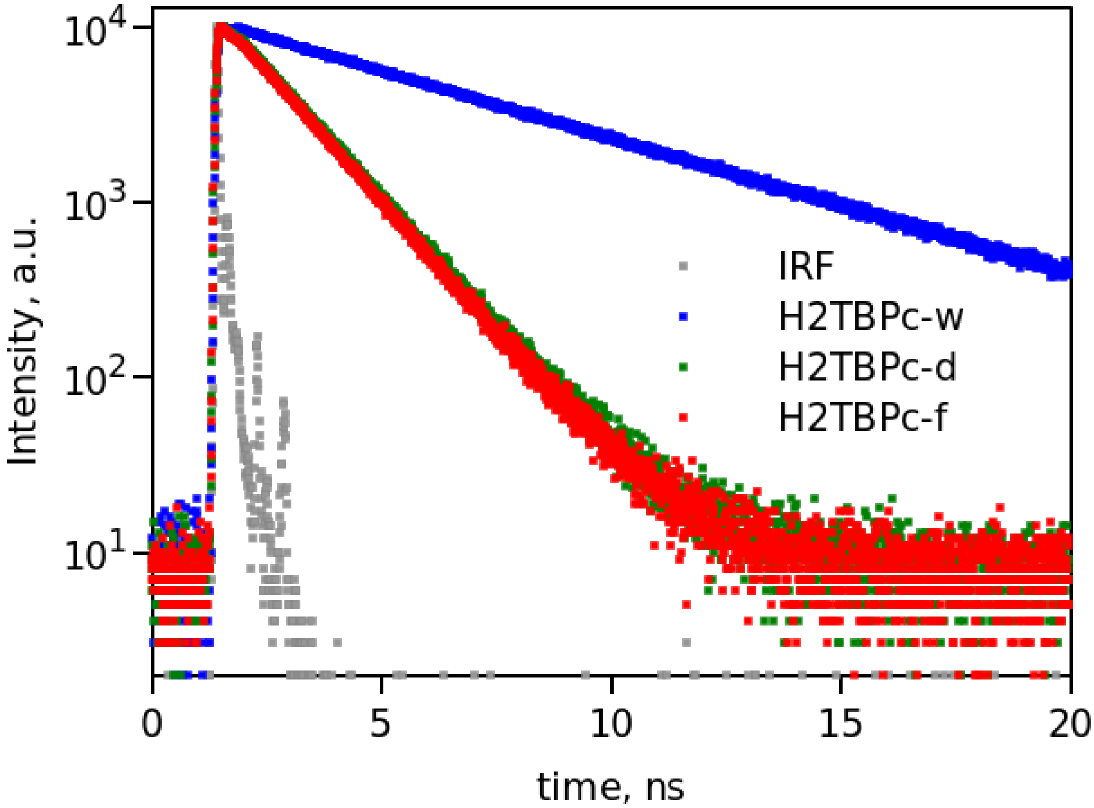

Fig. S14. Emission decays of **H_2Pc-Windmill**, **H_2Pc-Dragon**, and **H_2Pc-Frog** measured at the corresponding emission band maxima and excited at 375 nm. IRF is the instrument response function.

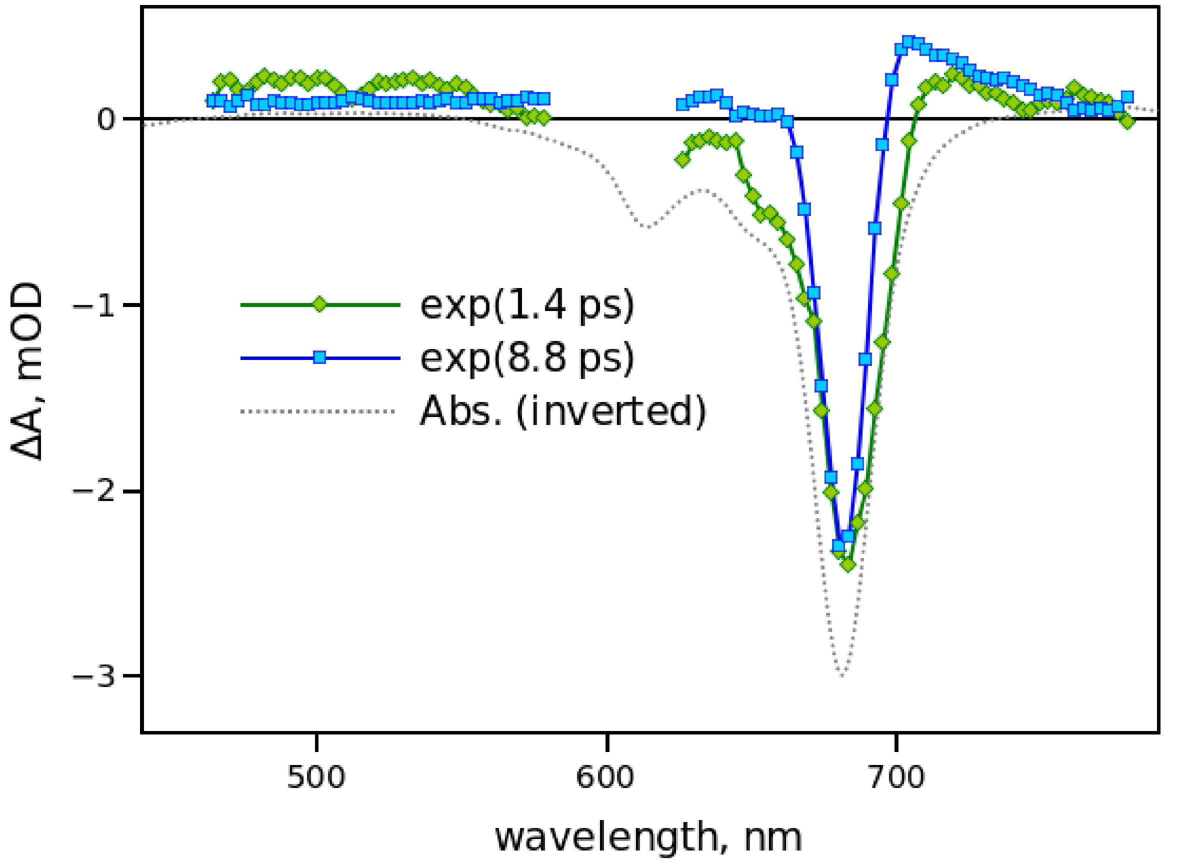

Fig. S15. DAS of **CoPc-Windmill** in toluene. The associated time constants are shown in the plot. The gray dotted line shows absorption spectrum inverted and scaled for comparison.

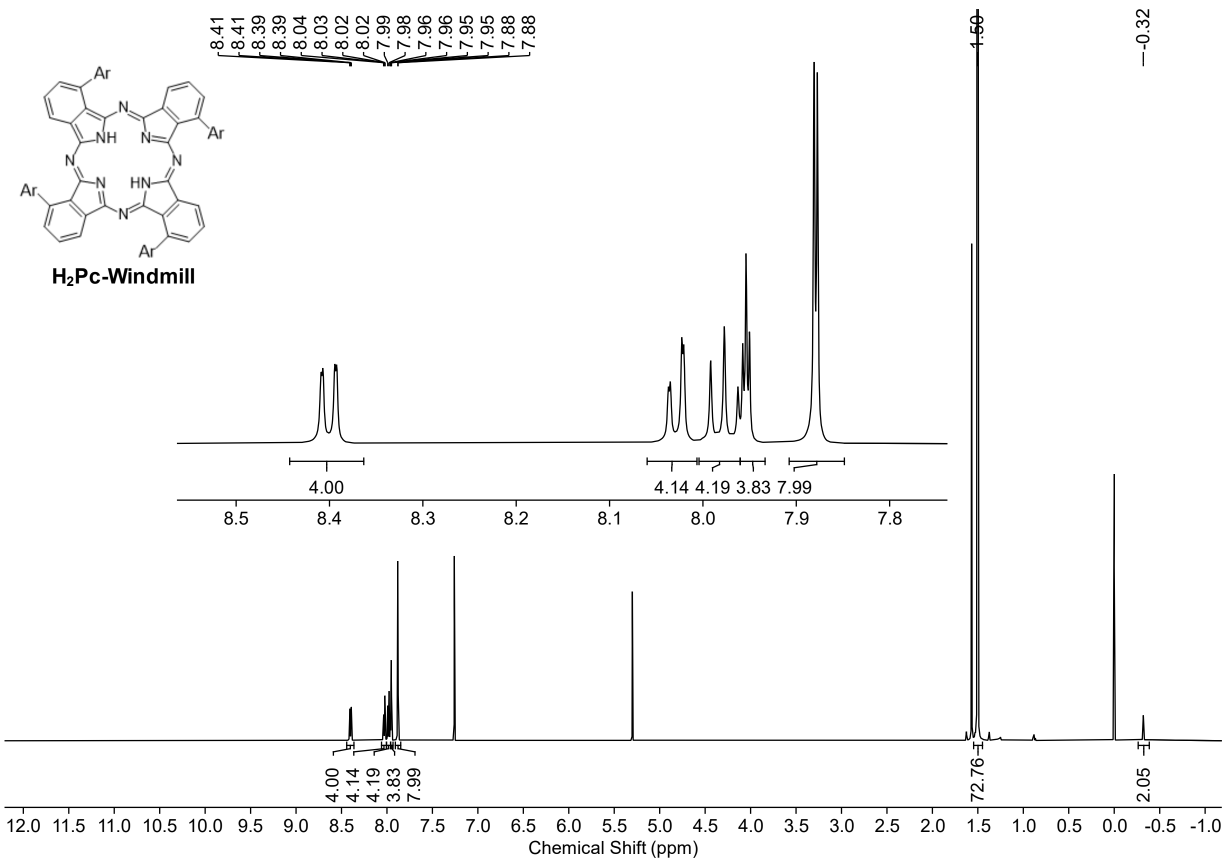

Fig. S16. ^{1}H NMR spectrum (500 MHz, $CDCl_3$) of **H_2Pc-Windmill**.

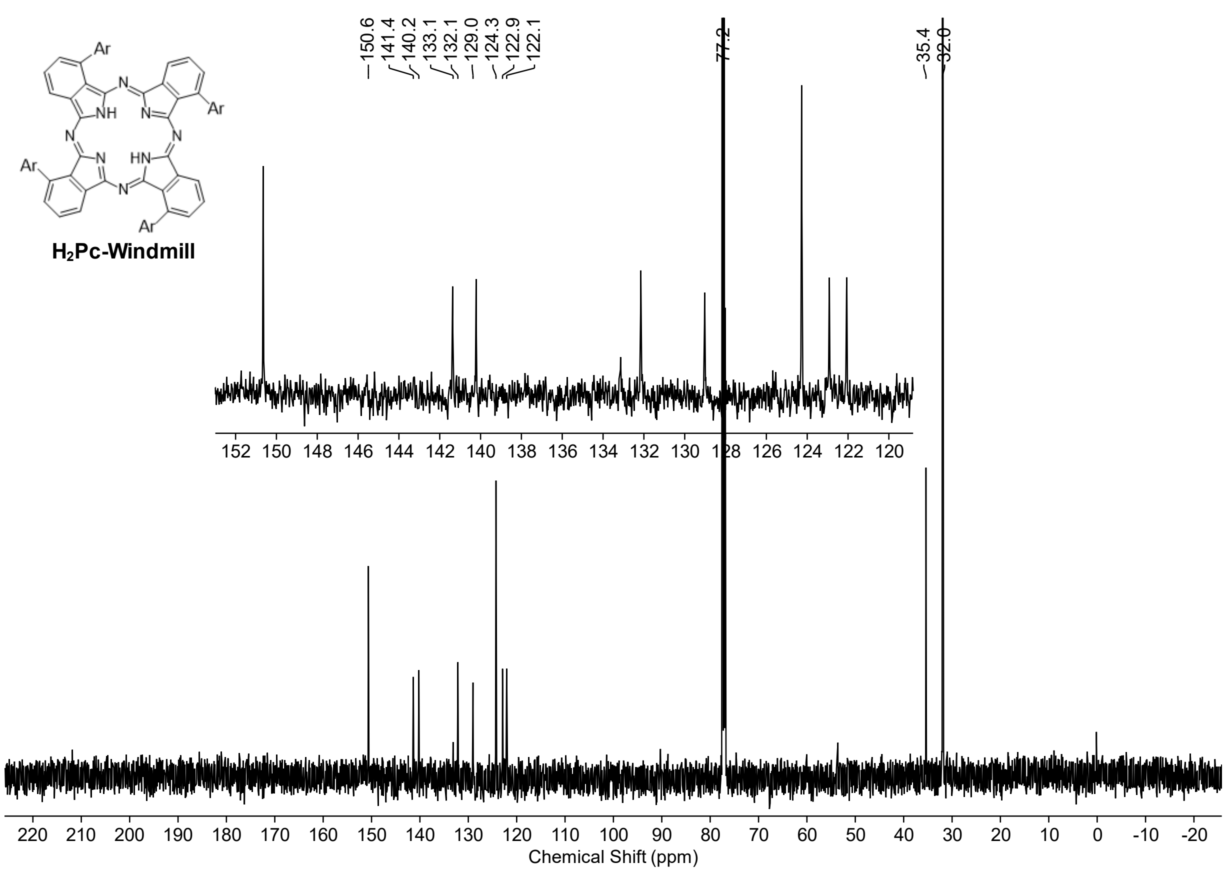

Fig. S17. ^{13}C{^{1}H} NMR spectrum (126 MHz, $CDCl_3$) of **H_2Pc-Windmill**.

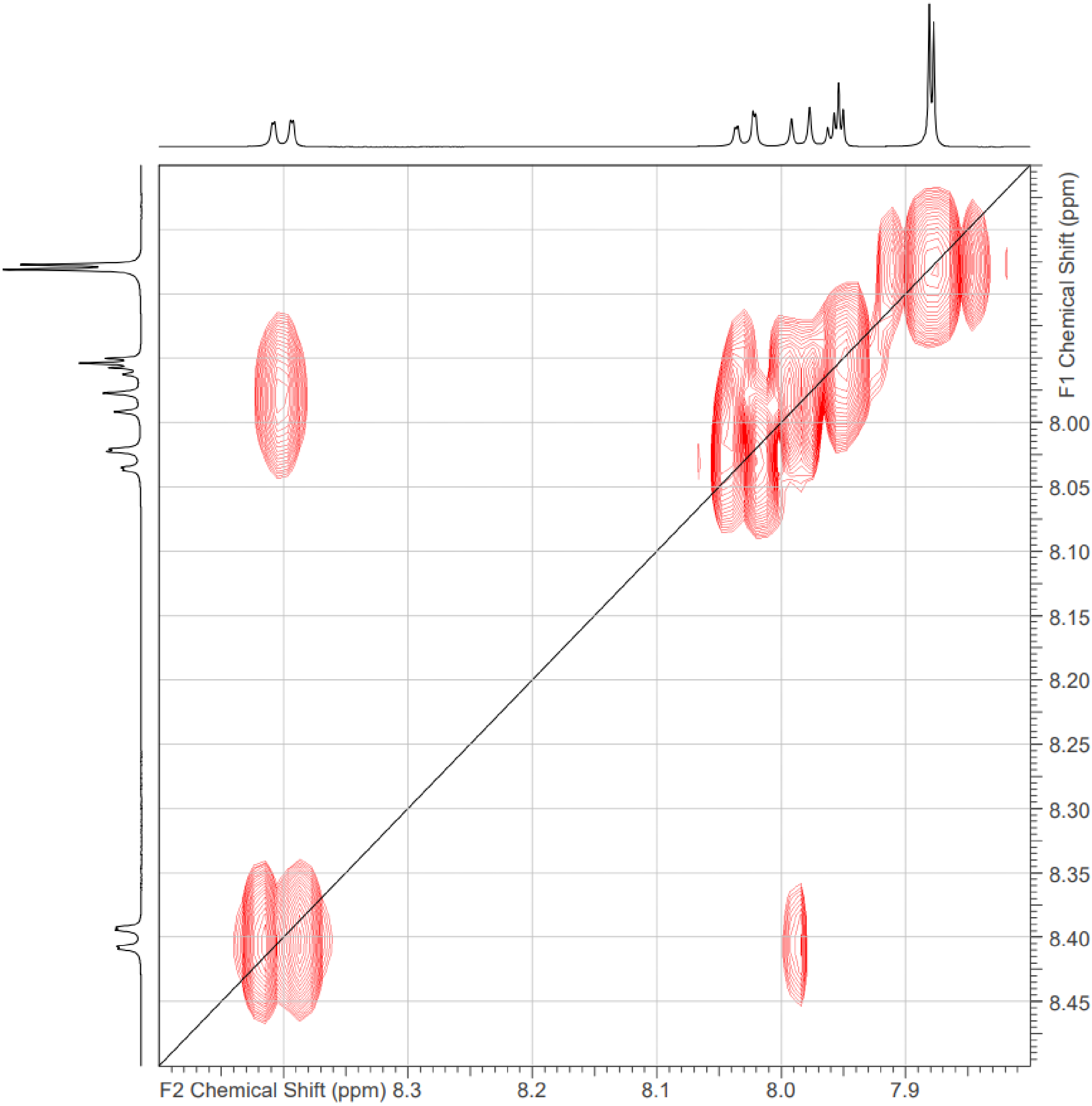

Fig. S18. ${}^{1}H$–${}^{1}H$ COSY NMR spectrum (500 MHz, $CDCl_3$) of **H_2Pc-Windmill**.

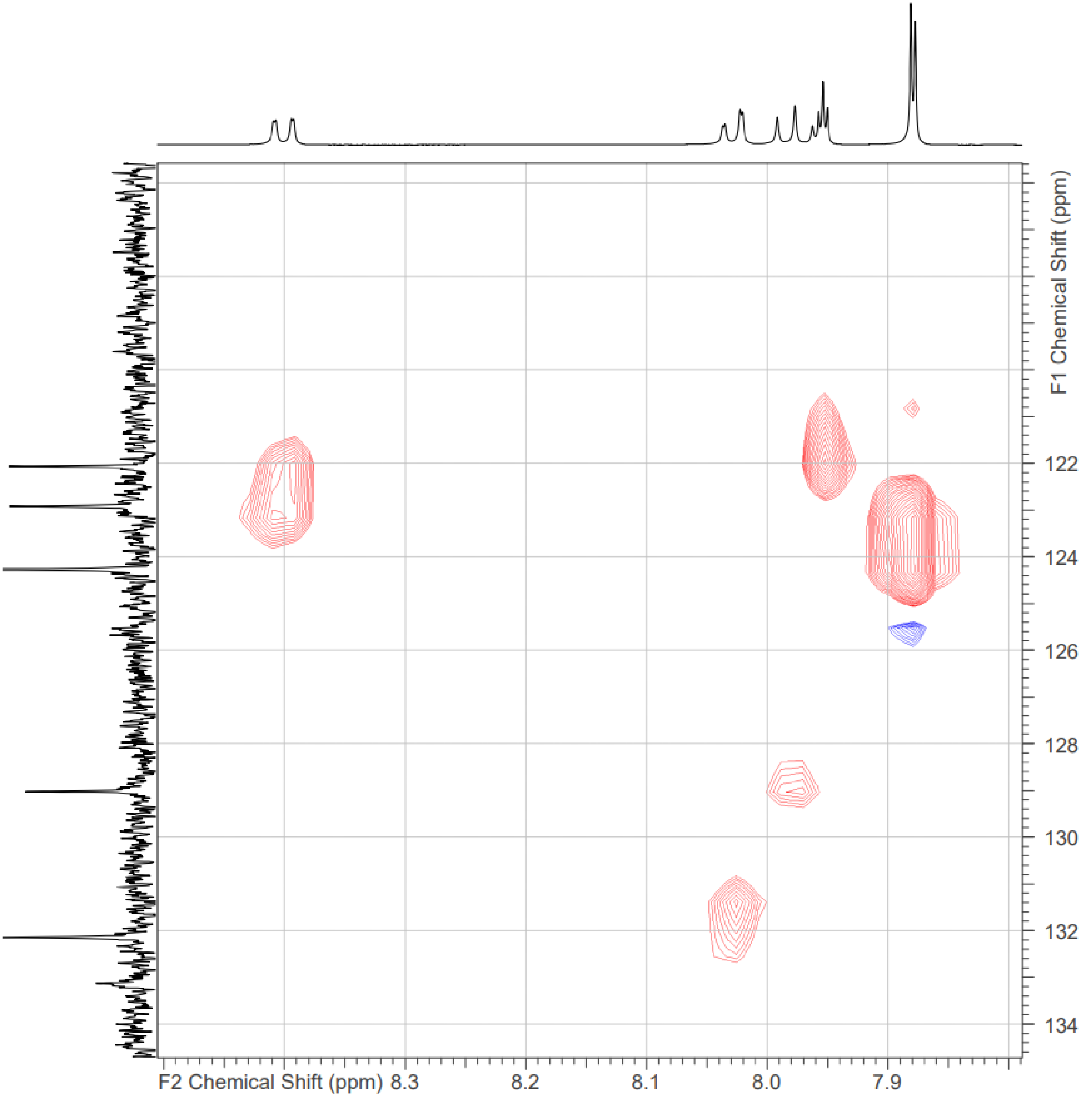

Fig. S19. ^{1}H–^{13}C HSQC NMR spectrum (500 MHz, $CDCl_3$) of **H_2Pc-Windmill**.

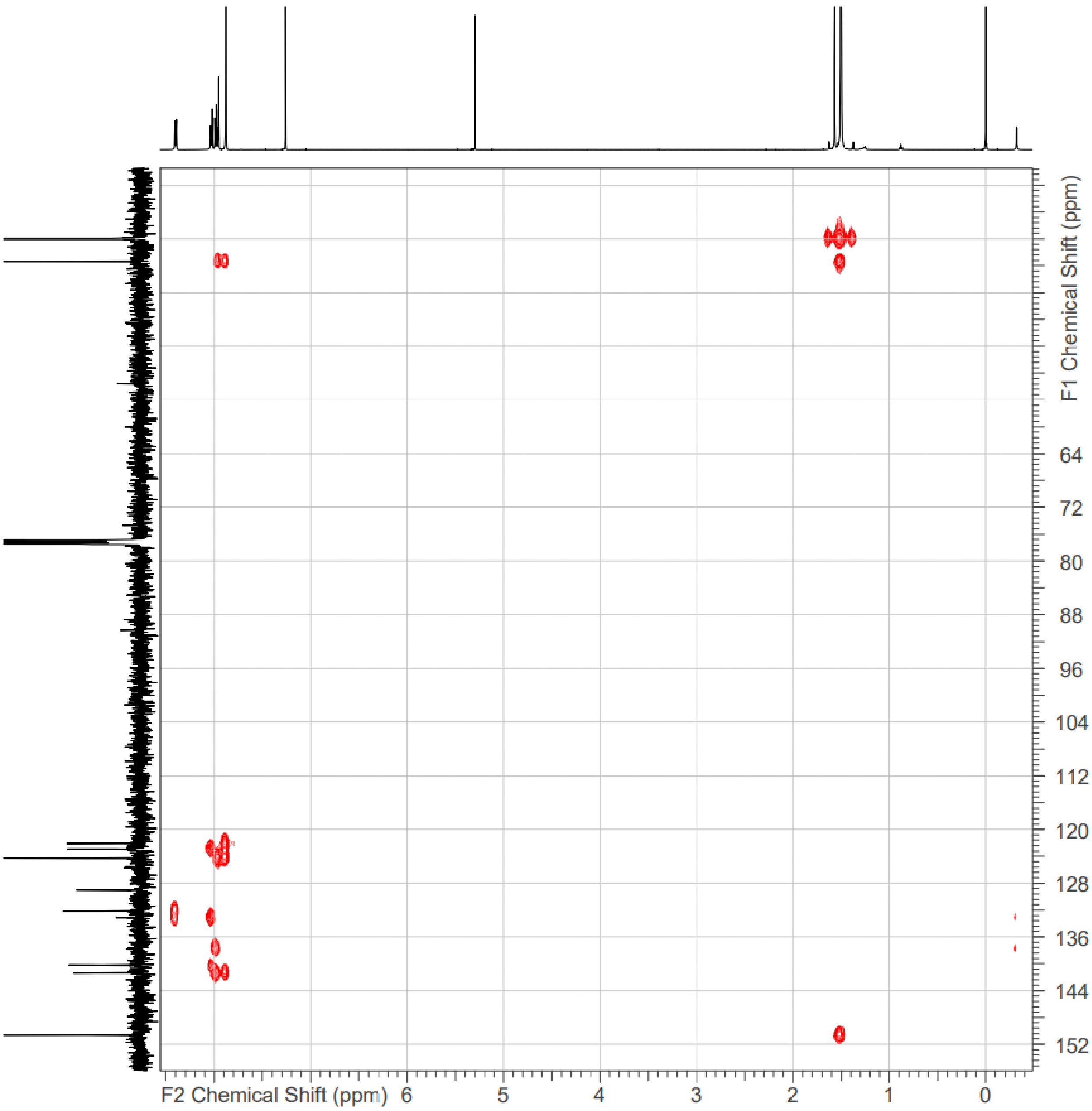

Fig. S20. ^{1}H–^{13}C HMBC NMR spectrum (500 MHz, $CDCl_3$) of **H_2Pc-Windmill**.

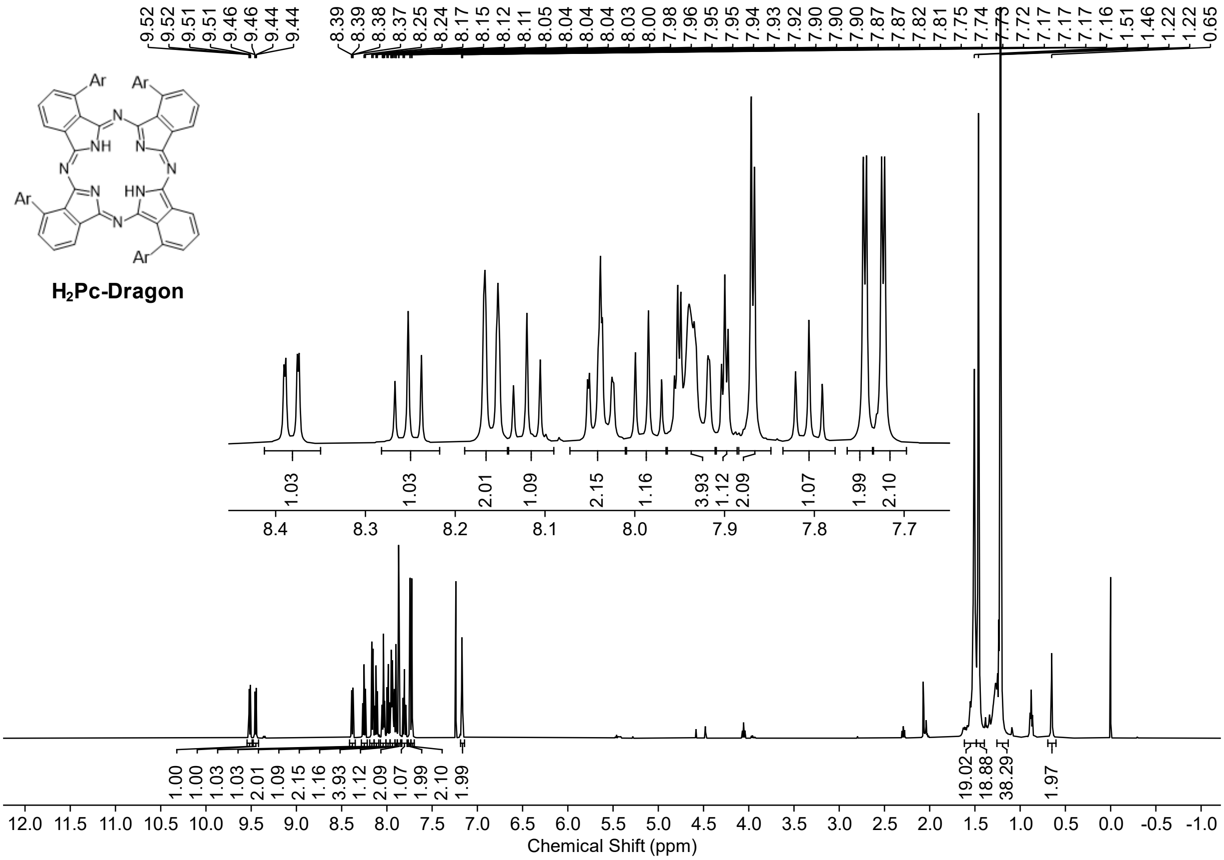

Fig. S21. ^{1}H NMR spectrum (500 MHz, $CDCl_3$) of **H_2Pc-Dragon**.

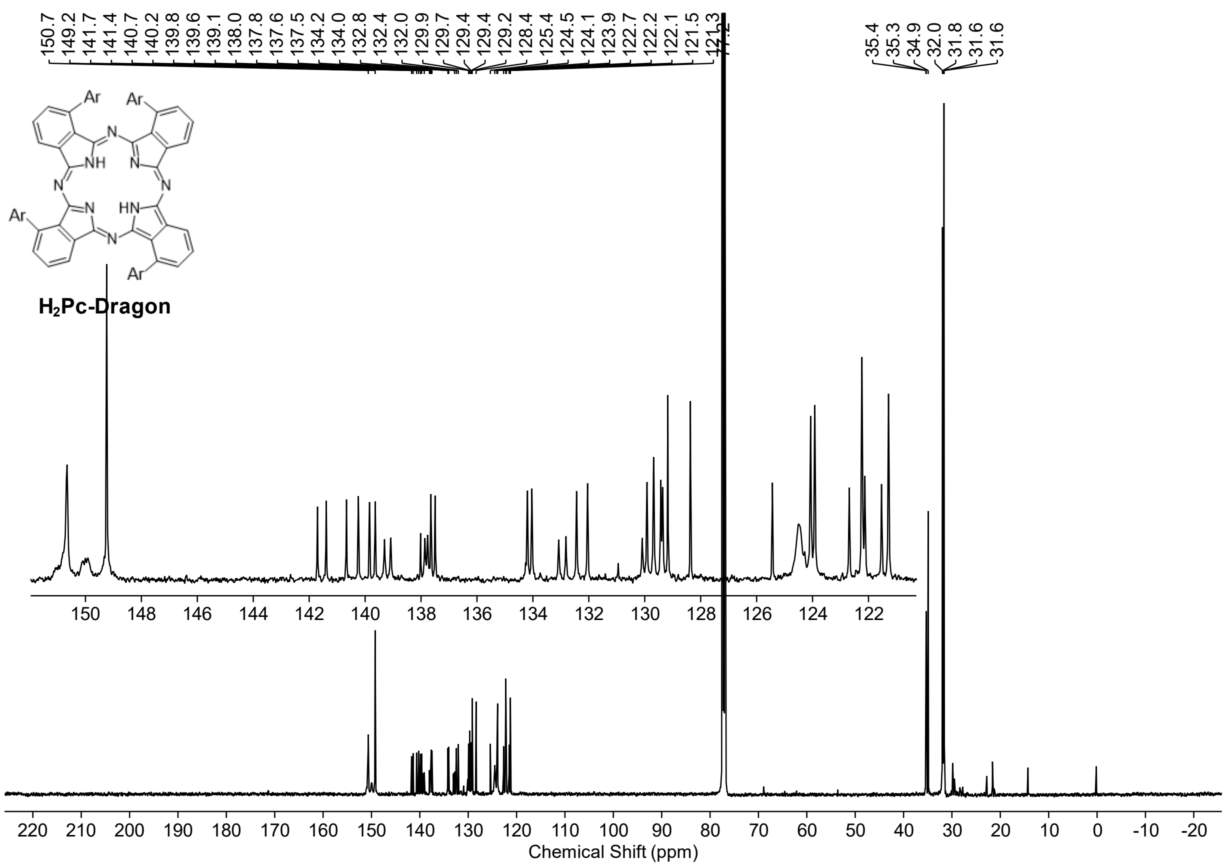

Fig. S22. $^{13}C\{^{1}H\}$ NMR spectrum (126 MHz, $CDCl_3$) of **H_2Pc-Dragon**.

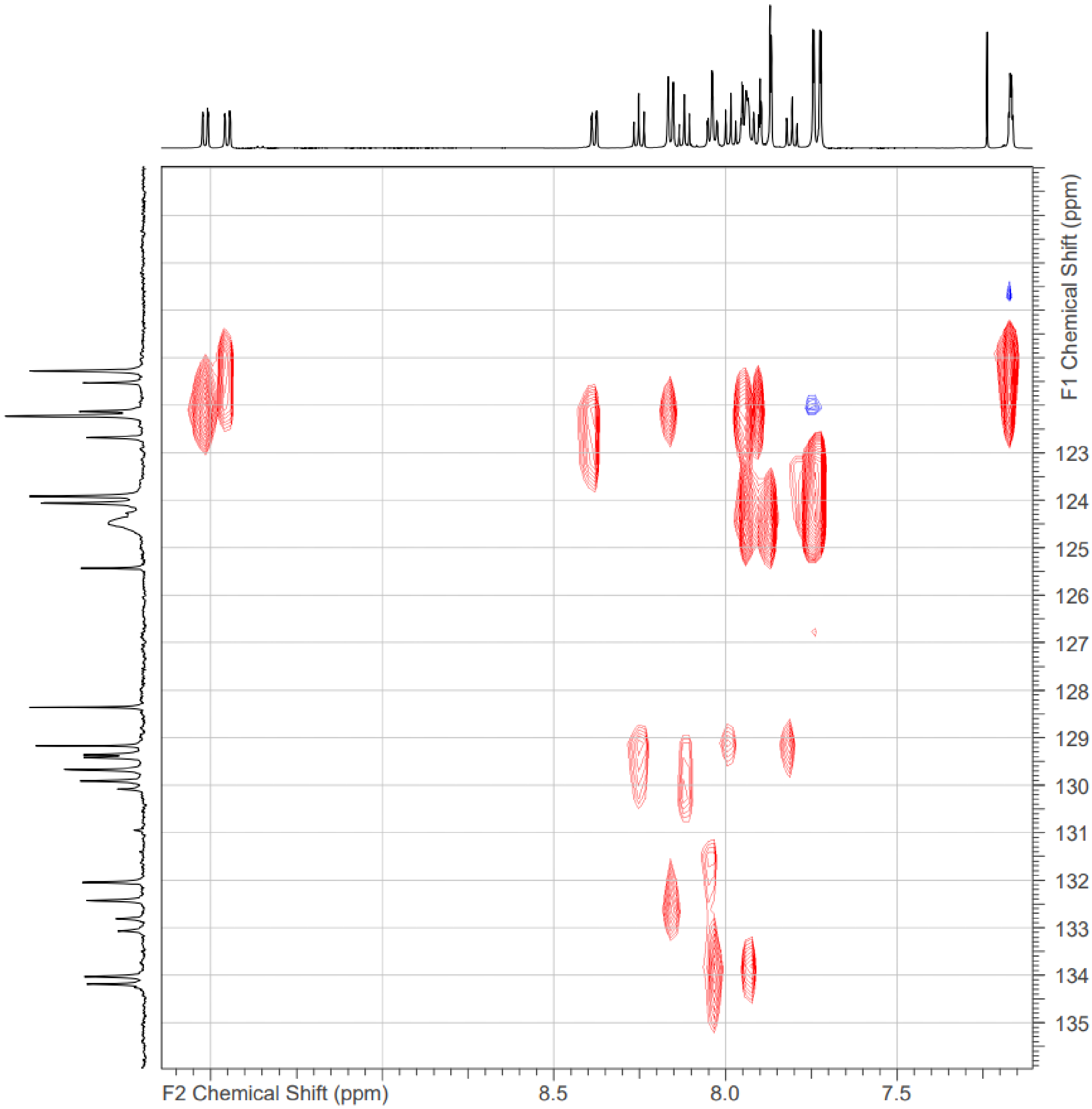

Fig. S23. ^1H–^{13}C HSQC NMR spectrum (500 MHz, $CDCl_3$) of **H_2Pc-Dragon**.

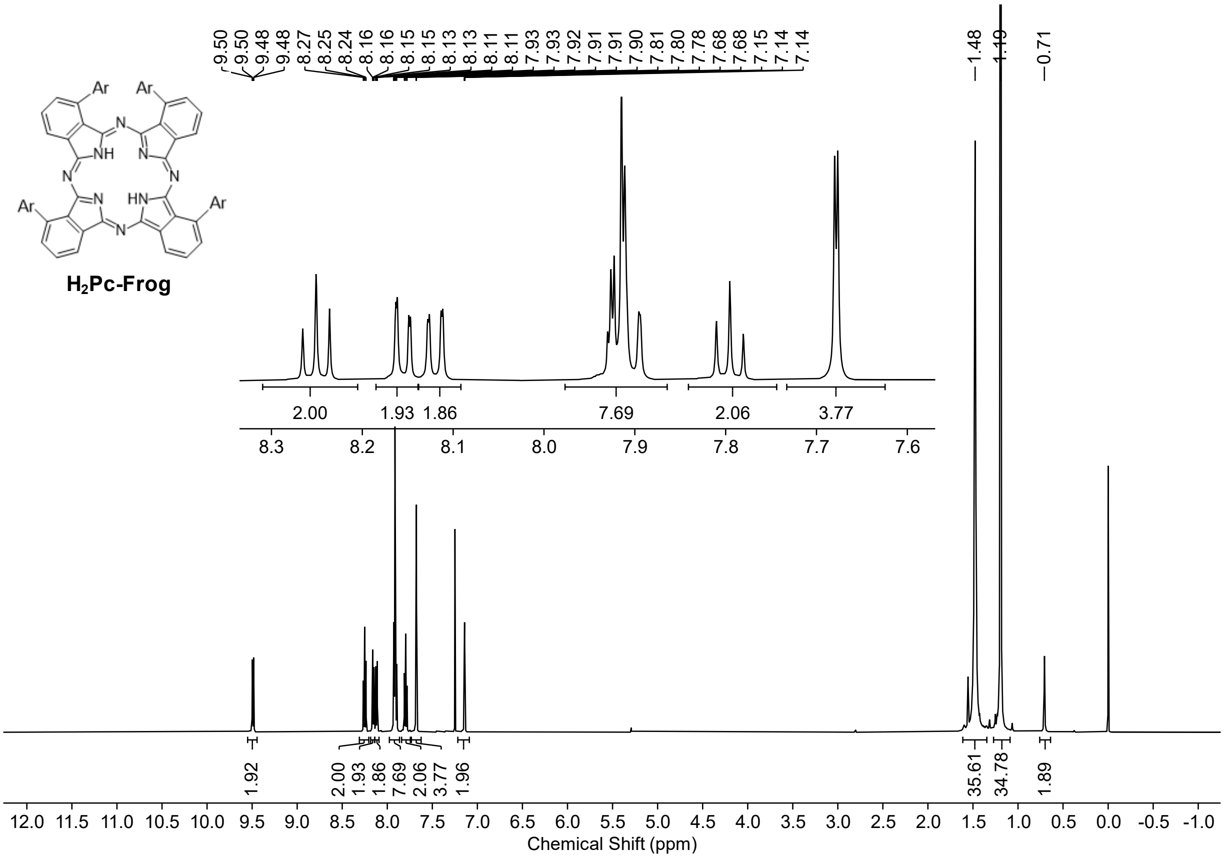

Fig. S24. ^{1}H NMR spectrum (500 MHz, $CDCl_3$) of **H_2Pc-Frog**.

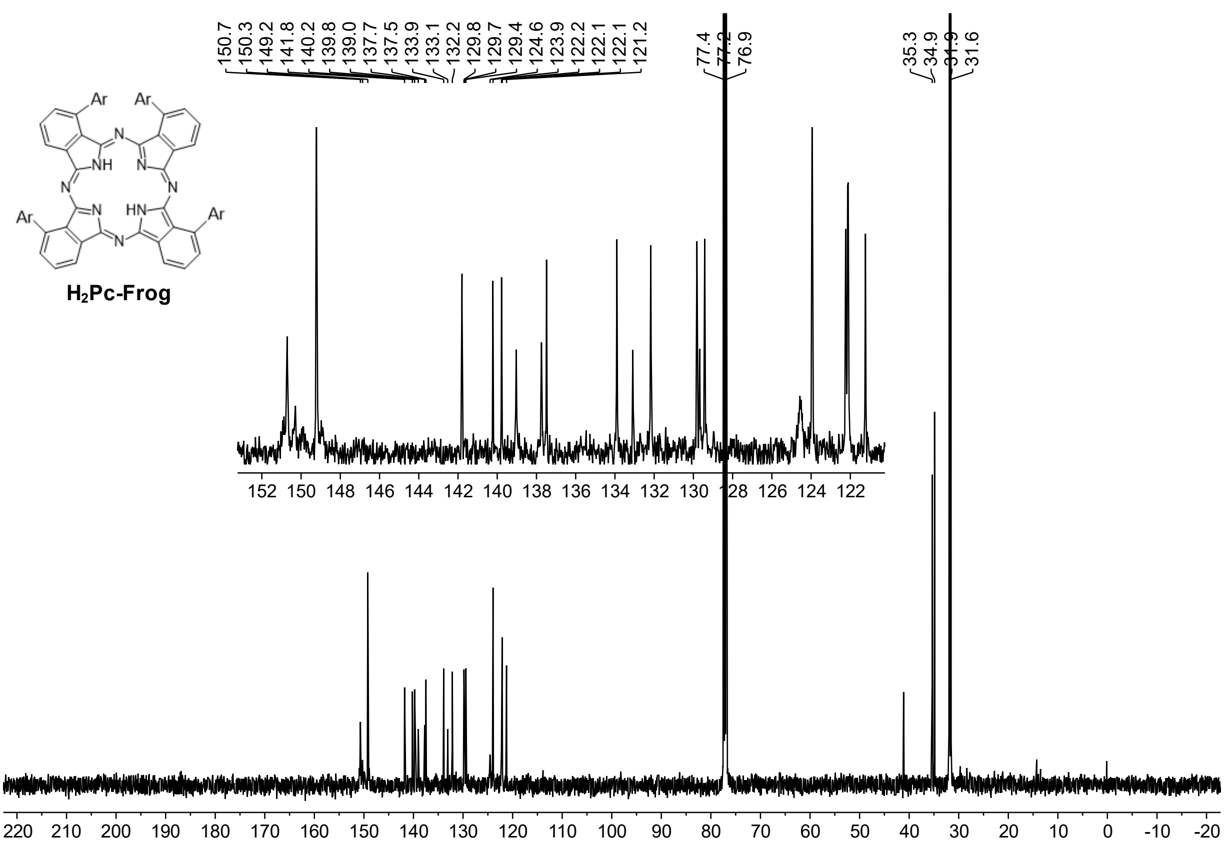

Fig. S25. $^{13}C\{^{1}H\}$ NMR spectrum (126 MHz, $CDCl_3$) of **H_2Pc-Frog**.

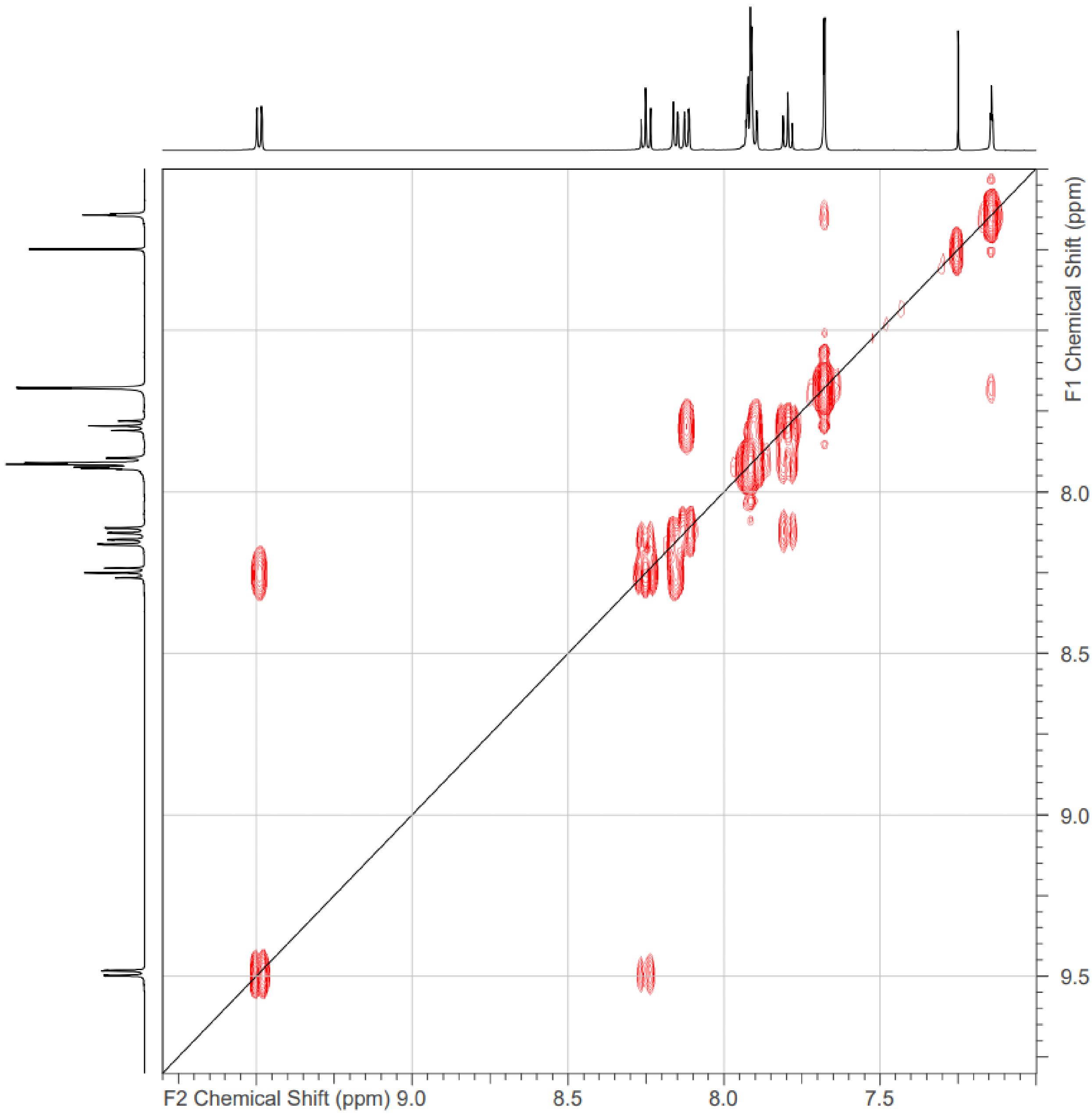

Fig. S26. ^1H–^1H COSY NMR spectrum (500 MHz, $CDCl_3$) of **H_2Pc-Frog**.

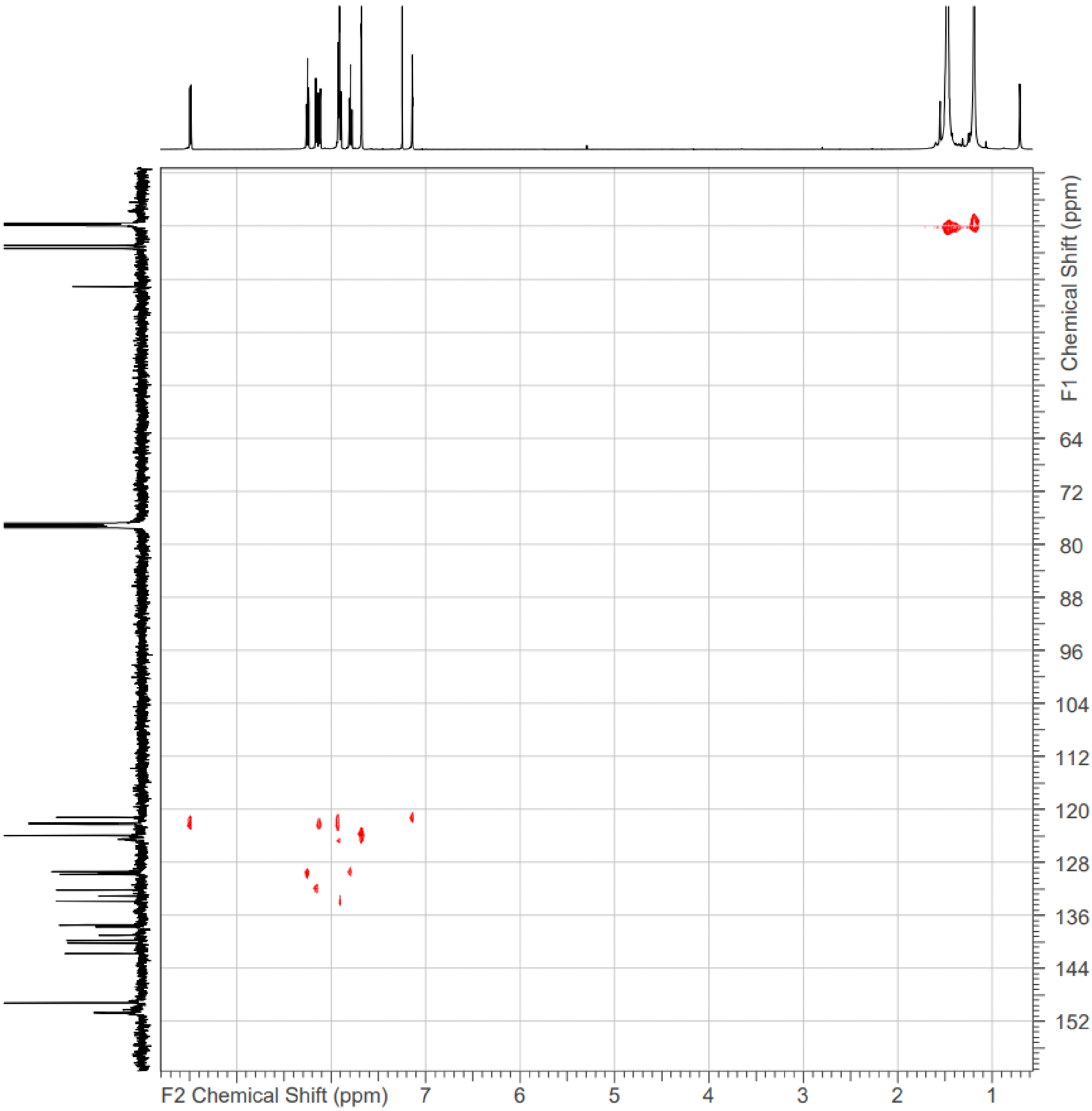

Fig. S27. ^{1}H–^{13}C HSQC NMR spectrum (500 MHz, $CDCl_3$) of **H_2Pc-Frog**.

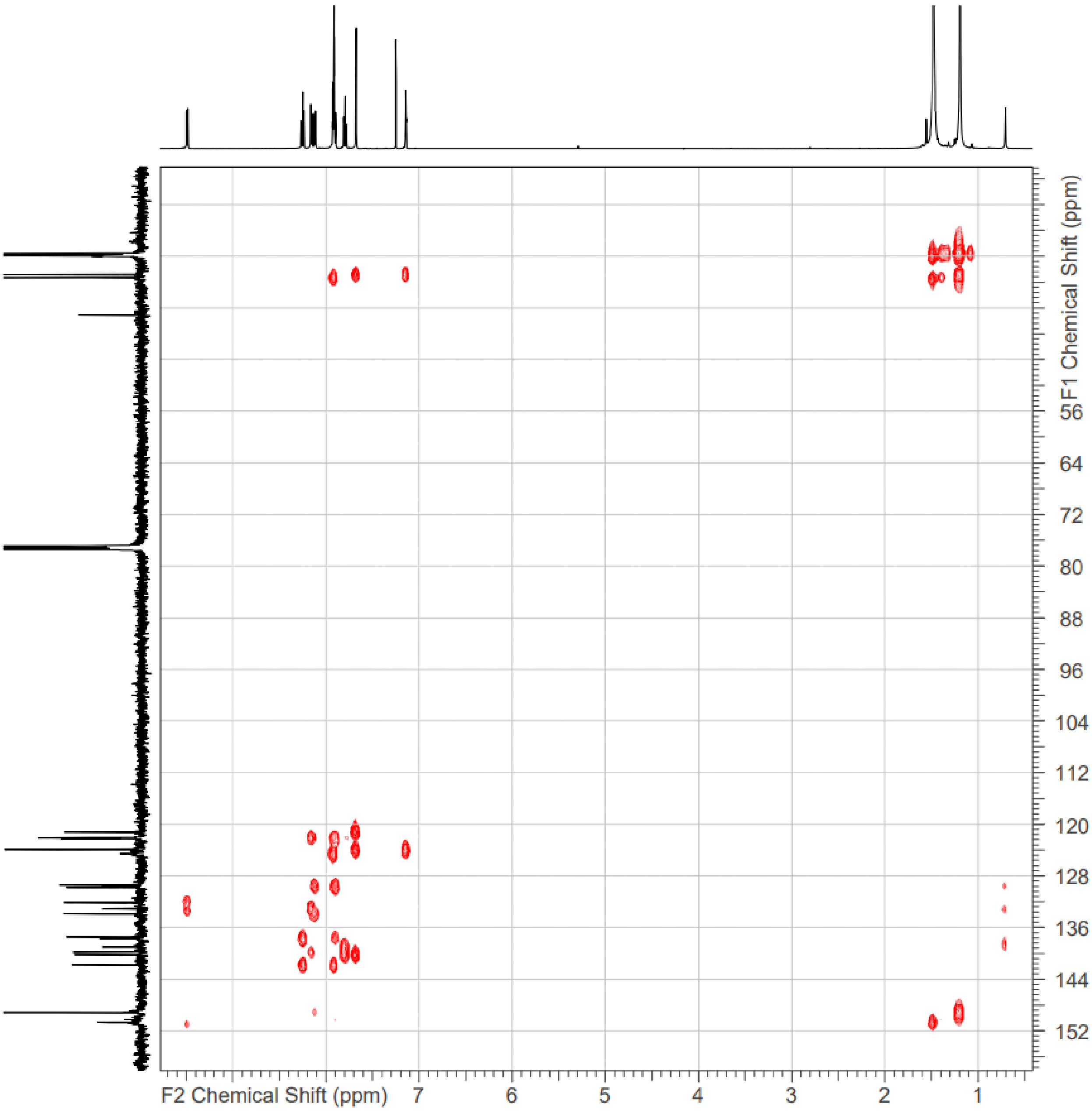

Fig. S28. [1]H–[13]C HMBC NMR spectrum (500 MHz, $CDCl_3$) of **H_2Pc-Frog**.

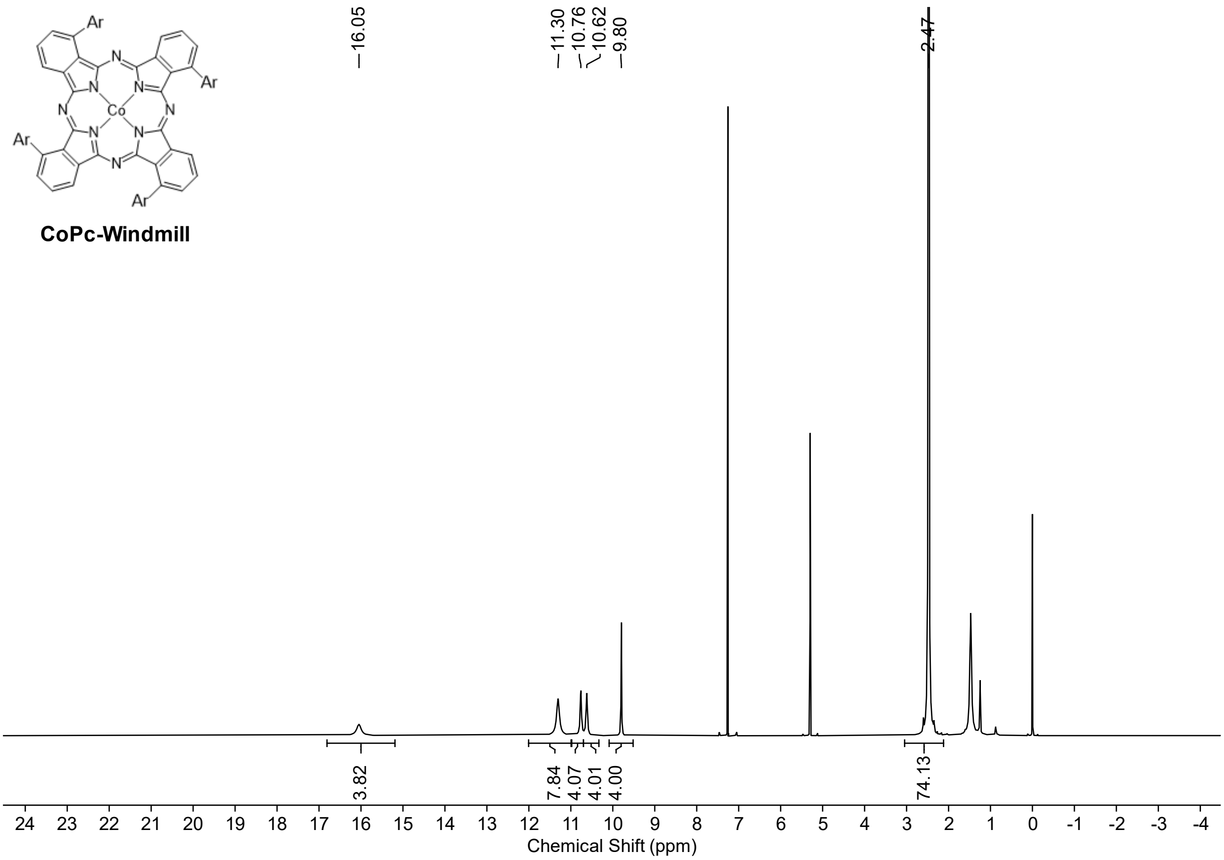

Fig. S29. ^{1}H NMR spectrum (500 MHz, $CDCl_3$) of **CoPc-Windmill**.

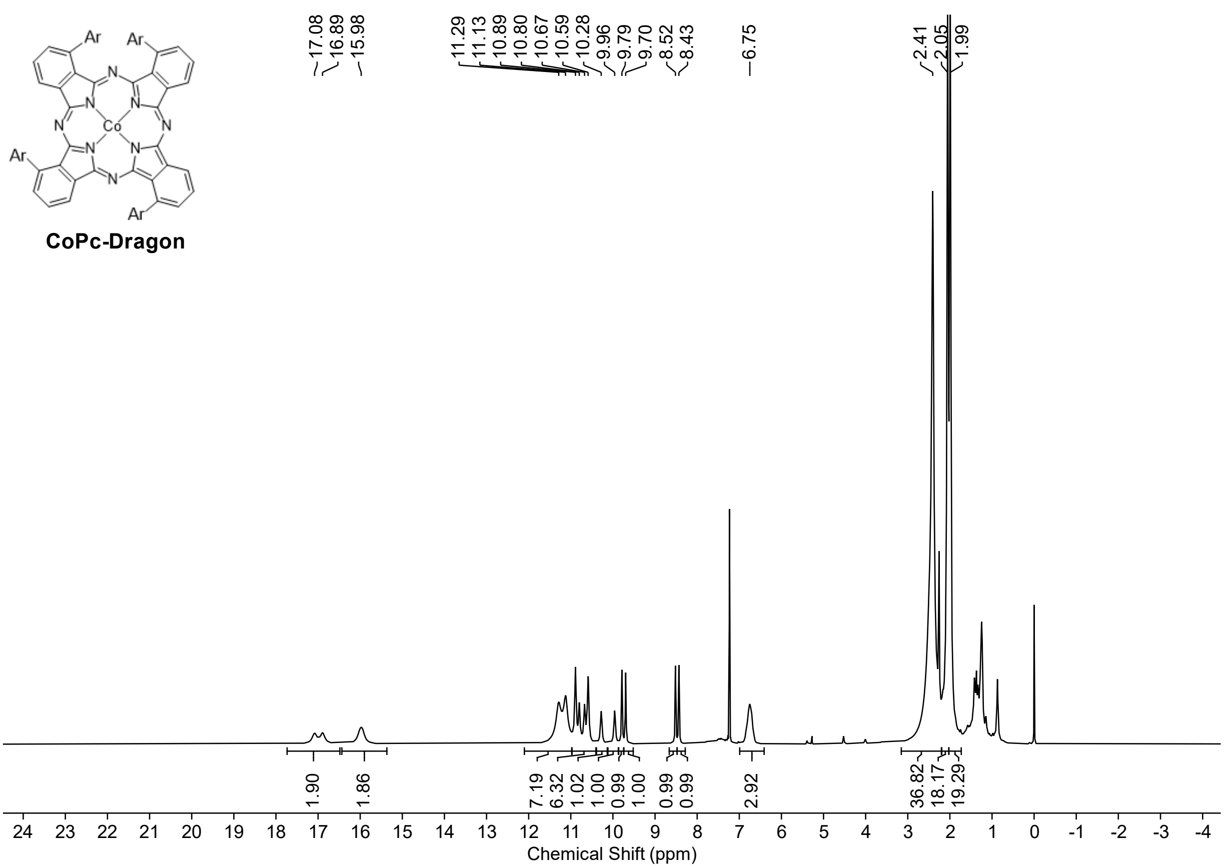

Fig. S30. ^{1}H NMR spectrum (500 MHz, $CDCl_3$) of **CoPc-Dragon**.

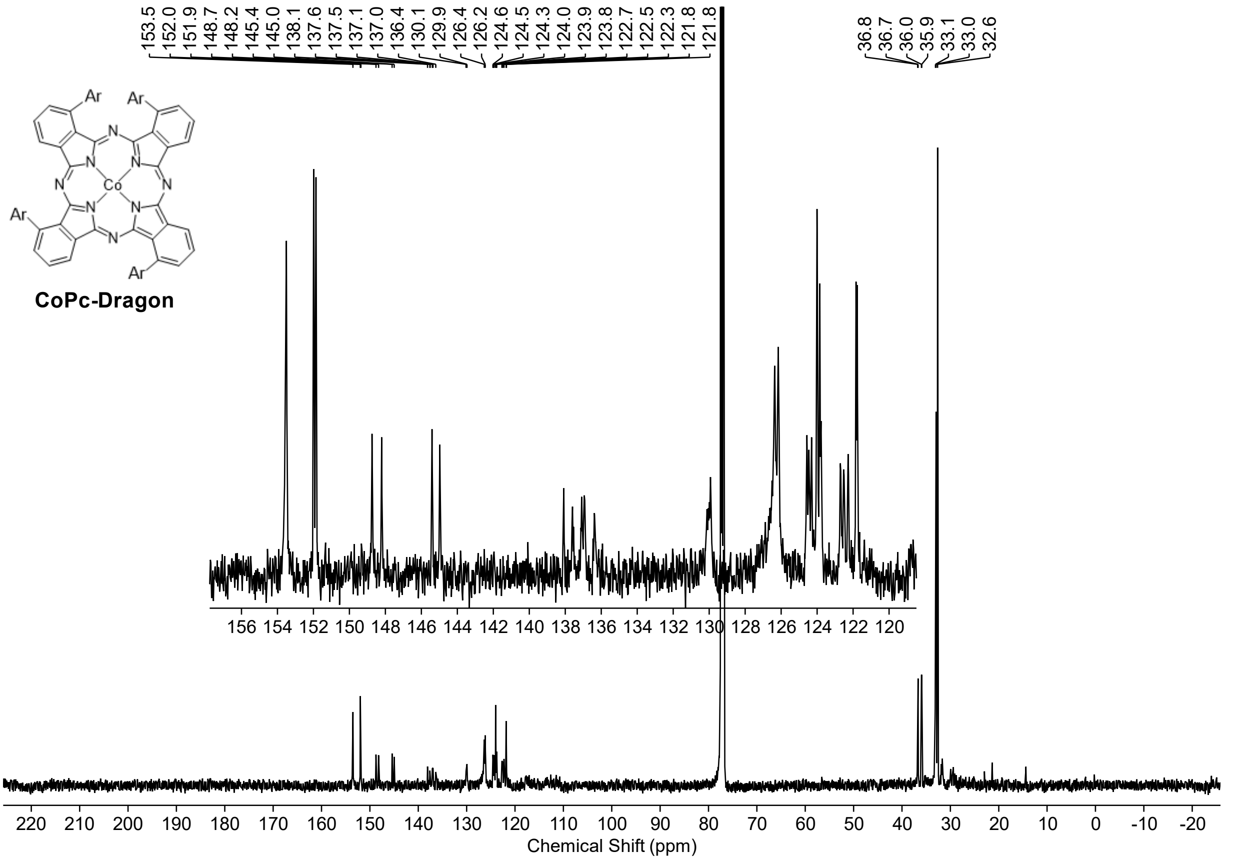

Fig. S31. $^{13}C\{^{1}H\}$ NMR spectrum (126 MHz, $CDCl_3$) of **CoPc-Dragon**.

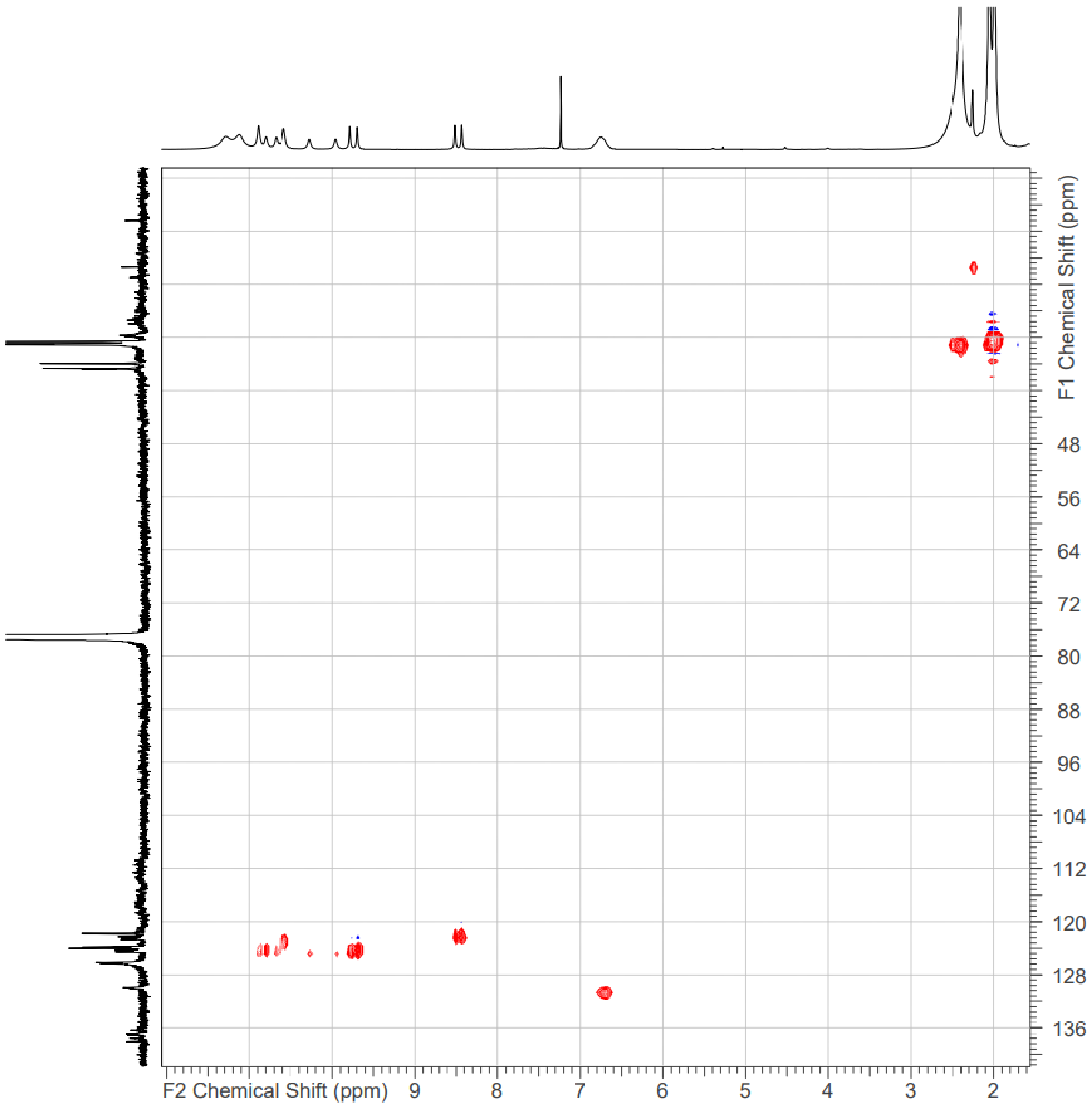

Fig. S32. ^{1}H–^{13}C HSQC NMR spectrum (500 MHz, $CDCl_3$) of **CoPc-Dragon**.

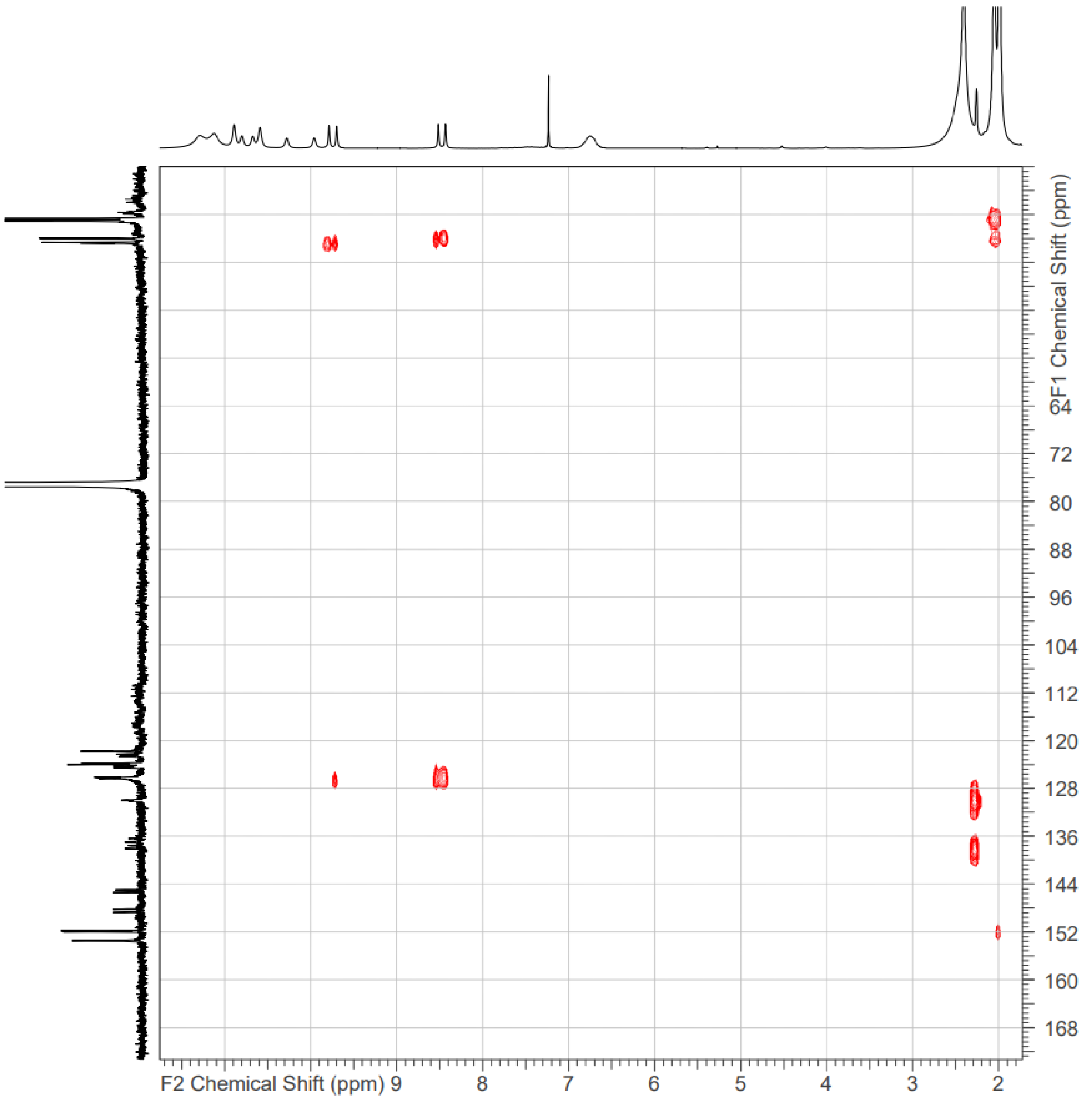

Fig. S33. ^{1}H–^{13}C HMBC NMR spectrum (500 MHz, $CDCl_3$) of **CoPc-Dragon**.

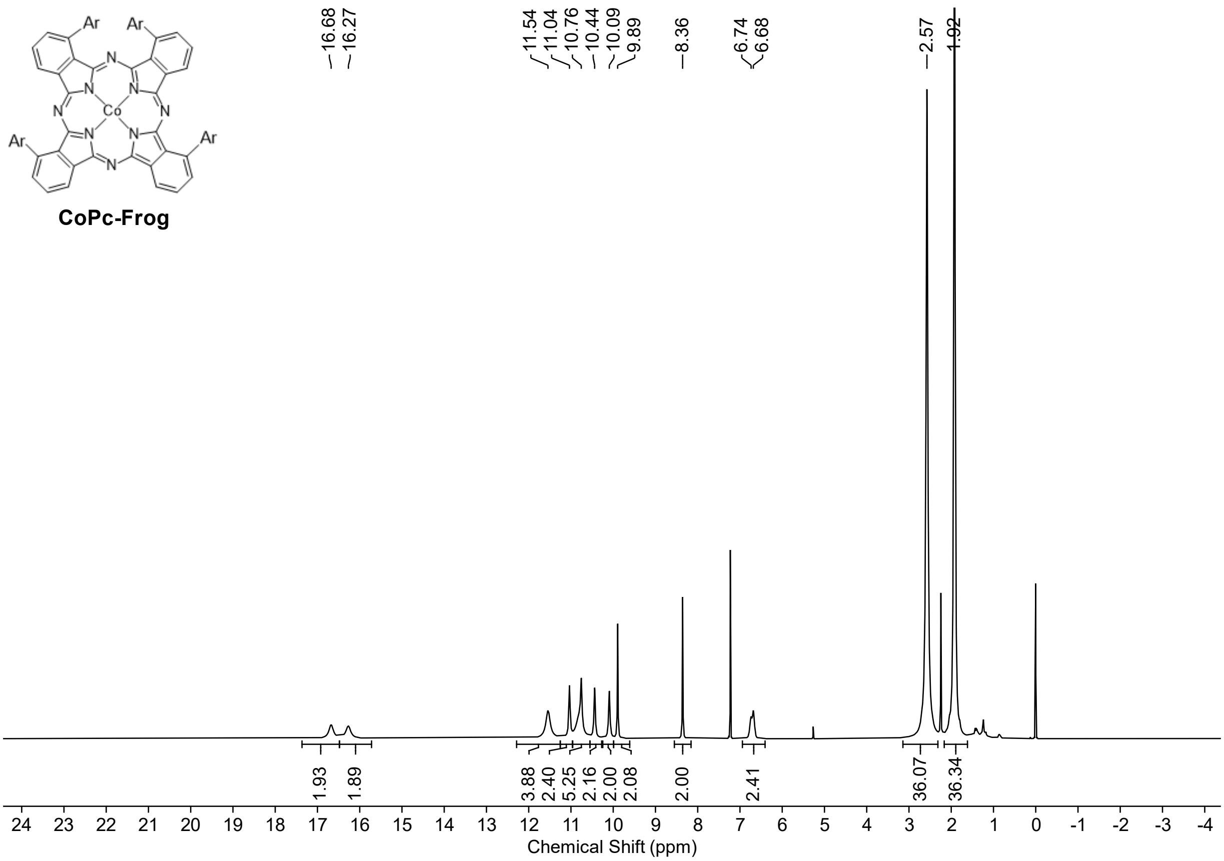

Fig. S34. ^{1}H NMR spectrum (500 MHz, $CDCl_3$) of **CoPc-Frog**.

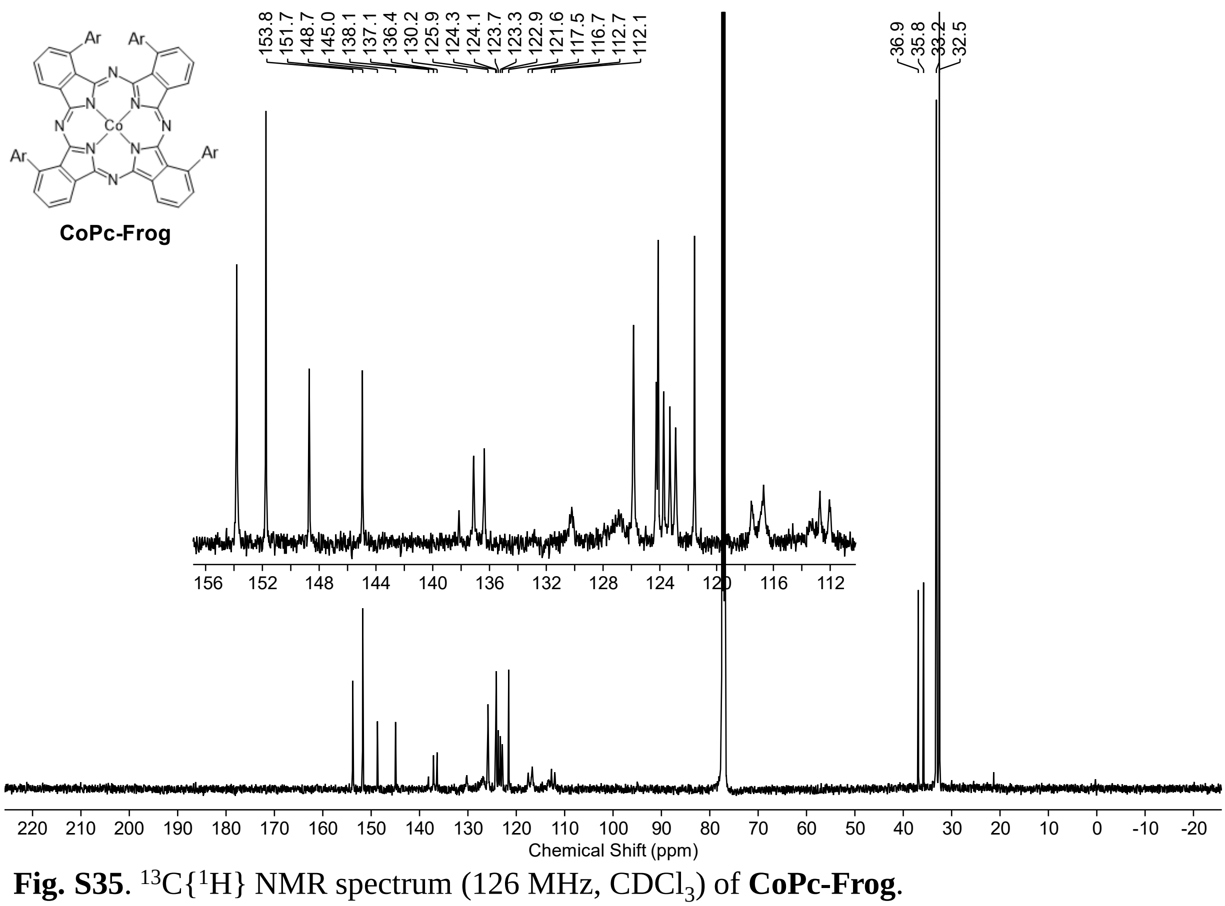

Fig. S35. $^{13}C\{^{1}H\}$ NMR spectrum (126 MHz, $CDCl_3$) of **CoPc-Frog**.

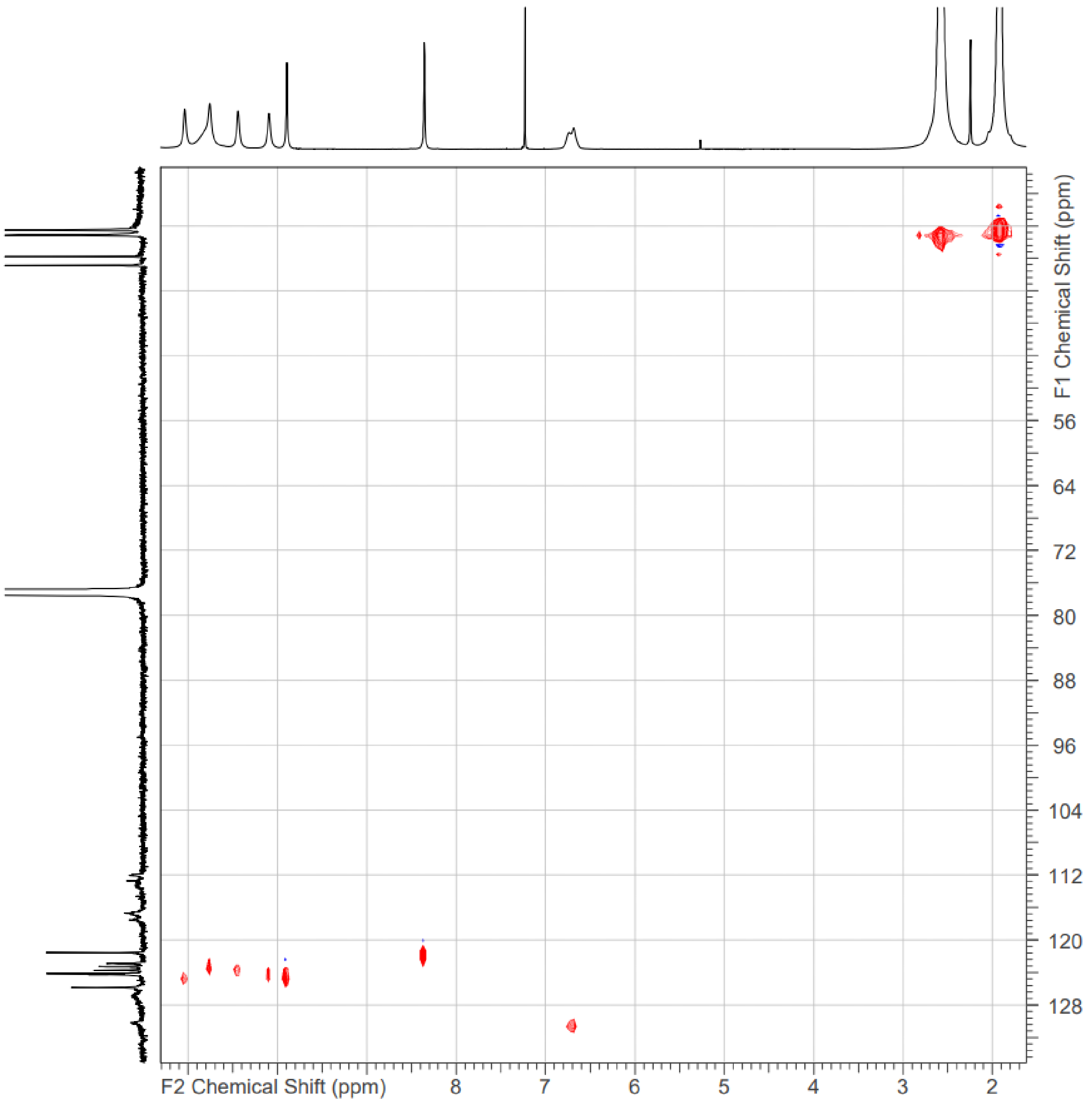

Fig. S36. ^{1}H–^{13}C HSQC NMR spectrum (500 MHz, $CDCl_3$) of **CoPc-Frog**.

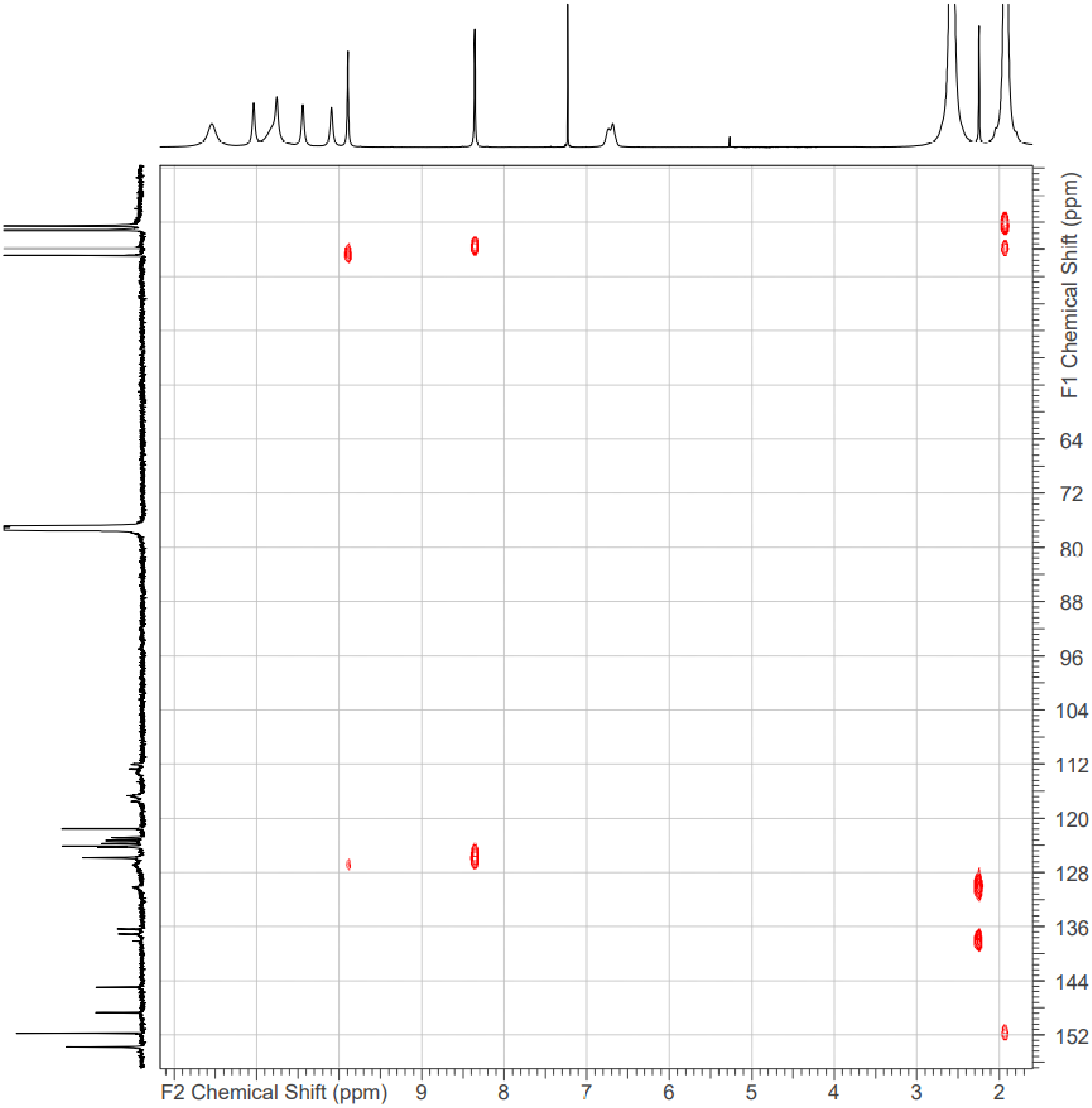

Fig. S37. ^1H–^{13}C HMBC NMR spectrum (500 MHz, $CDCl_3$) of **CoPc-Frog**.